Research Square

Preprints are preliminary reports that have not undergone peer review.
They should not be considered conclusive, used to inform clinical practice,
or referenced by the media as validated information.

An Age-Structured Analytics Model for Pneumonia Transmission and Vaccination Strategies

MD. Sohel Rana
Noakhali Science and Technology University
Sadia Akter Lima
Noakhali Science and Technology University
Zihad Hasan Riku
Noakhali Science and Technology University
Kamrunnesa Mayeda
Noakhali Science and Technology University
Md. Kamrujjaman
kamrujjaman@du.ac.bd

University of Dhaka

Research Article

Keywords: Age-structured modeling, Optimal control, Pneumonia, Disease dynamics, Sensitivity analysis, Public health

Posted Date: November 4th, 2026

DOI: https://doi.org/10.21203/rs.3.rs-11303638/v1

License: This work is licensed under a Creative Commons Attribution 4.0 International License.
Read Full License

Additional Declarations: No competing interests reported.

An Age-Structured Analytics Model for Pneumonia Transmission and Vaccination Strategies

MD. Sohel Rana [*1], Sadia Akter Lima [†1], Zihad Hasan Riku[‡1], Kamrunnesa Mayeda [§1], and Md. Kamrujjaman [¶ 2]

[1]Department of Applied Mathematics, Noakhali Science and Technology University, Noakhali-3814, Bangladesh
[2]Department of Mathematics, University of Dhaka, Dhaka-1000, Bangladesh

Abstract. Pneumonia remains a major public health concern worldwide, with millions of new cases reported each year. In this study, we develop a modified mathematical model to describe the transmission dynamics of pneumonia with vaccination and analyze the spread of infection across three age groups: under 5 years, 5–64 years, and above 64 years. First, we compute the basic reproduction number $R_0 = 0.298$, which indicates that the disease cannot sustain transmission within the population across all age groups. In addition, we study the local and global stability and perform a global sensitivity analysis in terms of R_0, which shows how key parameters are important in preventing disease transmission. We examine the model by comparing system dynamics under two scenarios: with vaccination and without vaccination. An optimal control framework is introduced with two control variables representing a balanced diet and improved hygiene practices. By applying Pontryagin's Maximum Principle, we derive the optimal control strategies and characterize the corresponding optimal control profiles for the three age groups. Numerical simulations show graphically that vaccination combined with additional control measures can significantly reduce pneumonia incidence, demonstrate how the parameters vary, and compare the cost-effectiveness of the two introduced control measures. The results suggest that vaccination alone is particularly effective for children under 5 years, whereas for 5–64 years and above 64 years, the combined implementation of vaccination and the two control strategies provides the greatest reduction in disease burden. These findings highlight the importance of targeted immunization programs, along with supportive health interventions such as improved nutrition and hygiene, in reducing pneumonia prevalence and preventing future outbreaks.

Keywords: Age-structured modeling; Optimal control; Pneumonia; Disease dynamics; Sensitivity analysis; Public health.
AMS Subject Classification 2020: 92D30, 37N25, 92D40, 93E03.

[*]E-mail: sr907815@gmail.com, Phone: +880 1627201629
[†]E-mail: sadia.amath@nstu.edu.bd, Phone: +880 1701451426
[‡]E-mail: zihadhassan2015@gmail.com, Phone: +880 1735356629
[§]E-mail: kamrunnesamayeda@gmail.com, Phone: +880 1776-147424
[¶]Corresponding author E-mail: kamrujjaman@du.ac.bd, Phone: +880 1553458910

Highlights

1. Develop an age-structured analytics model to study pneumonia transmission and vaccination impact.
2. Evaluate vaccination, nutrition, and hygiene strategies using optimal control analytics.
3. Analyze key epidemiological parameters through global sensitivity analysis.
4. Demonstrate age-specific intervention effects on pneumonia transmission dynamics.
5. Identify targeted vaccination and prevention strategies to reduce pneumonia burden across age groups.

1 Introduction

Infectious diseases arise from viruses, bacteria, fungi, or parasites, and they commonly spread through environmental contamination or direct contact between individuals. As a result of these infections, the most common symptoms include fever, fatigue, and cough, although these may vary depending on the type of infection and the organs involved. In this context, widely observed infectious diseases include COVID-19, HIV, tuberculosis, influenza, and pneumonia. These diseases affect not only individual health but also place a heavy burden on public health systems by increasing hospitalization, causing long-term health complications, and, in severe situations, leading to early death. They also affect social and economic activities by reducing productivity, increasing healthcare expenses, and straining limited medical resources, especially in developing countries. For these reasons, infectious diseases remain a serious global health issue that demands continuous monitoring, prevention, and control.

An infectious disease, which is a respiratory infection that causes inflammation in the lungs, is known as pneumonia [1, 2]. Notably, it attacks the tiny air sacs, which are called alveoli. Pneumonia occurs when germs infect the lungs and cause inflammation. This inflammation happens when the body's natural defense goes into action against these infections. Inflammation might cause alveoli to fill up with fluid. This infection is mainly transmitted by air or direct contact with an infected person, or sometimes from microorganisms. When an infected person coughs, sneezes, or talks, pneumonia can spread through droplets in the air. Furthermore, it can be transmitted by physical contact. In rare cases, pneumonia can be caused by mosquitoes. Bacterial infections increase the risk of pneumonia. Pneumonia spreads rapidly in crowded or poorly ventilated spaces. The symptoms are common and include fever, chest pain, difficulty breathing, and cough. Though some groups are especially sensitive, the impact of pneumonia presents a major health hazard to all age groups. Young children under 5 years are especially vulnerable to serious respiratory infections because of their undeveloped immune systems. If adults between the ages of 5 and 64 have underlying medical issues, including diabetes, asthma, or compromised immunity, they may be more vulnerable. Those above 64 years have the highest risk, though, since aging naturally reduces the immune response and makes it more difficult to fight off diseases, including pneumonia. Reducing the effect of pneumonia in these sensitive groups depends critically on early identification, preventative actions, and healthcare accessibility [3].

There are 30 pathogens that are responsible for pneumonia. Moreover, the primary types are: bacterial pneumonia, viral pneumonia, fungal (mold) pneumonia, and aspiration pneumonia. The most common bacterial pneumonia is caused by Streptococcus pneumoniae, which occurs when the body becomes weak due to illness or other factors like malnutrition, aging, or a weak immune system due to the attack of bacteria. Additionally, CAP (community-acquired pneumonia) occurs due to Haemophilus influenzae, Chlamydia pneumoniae, and Legionella. Similar to rhinoviruses, coronaviruses, influenza, RSV, adenoviruses, and parainfluenza, viral pneumonia can also be caused by viruses, which are sometimes responsible for developing bacterial pneumonia. Next is fungal (mold) pneumonia, which is caused by Cryptococcus, Pneumocystis jirovecii, and Coccidioides fungus. People who have low immunity are most likely to suffer from this uncommon type of pneumonia. Another type, aspiration pneumonia, is caused by a lung infection, which is the result of solid or liquid food, spit, or vomit abruptly entering the lungs. Last but not least, hospital-acquired pneumonia occurs as a result of prolonged hospitalization, normally caused by antibiotic-resistant bacteria. In ancient times, pneumonia was also known as "winter fever," and the symptoms of this disease were described by the great physician Hippocrates around 460 BC. However, before the 19th century, pneumonia was identified as a bacterial disease. After that, in 1938, viral pneumonia was first described, making a significant advancement in understanding its causes and treatments [4].

Table 1: Worldwide death cases for three different age groups due to pneumonia between 2012 and 2024, [3] and [5].

Years	Under 5 years	5-64 years	Above 64 years	Total
2012	955043	562326	1 million	2.5 million
2013	937522	568298	1.05 million	2.55 million
2014	906682	574437	1.09 million	2.57 million
2015	874799	585369	1.12 million	2.58 million
2016	834601	599118	1.14 million	2.58 million
2017	787962	600666	1.18 million	2.57 million
2018	738405	613421	1.21 million	2.56 million
2019	693129	619541	1.24 million	2.55 million
2020	556987	581108	1.14 million	2.28 million
2021	501910	570387	1.11 million	2.18 million
2022	470,000	560,000	1.08 million	2.11 million
2023	440,000	555,000	1.07 million	2.07 million
2024	410,000	550,000	1.06 million	2.02 million

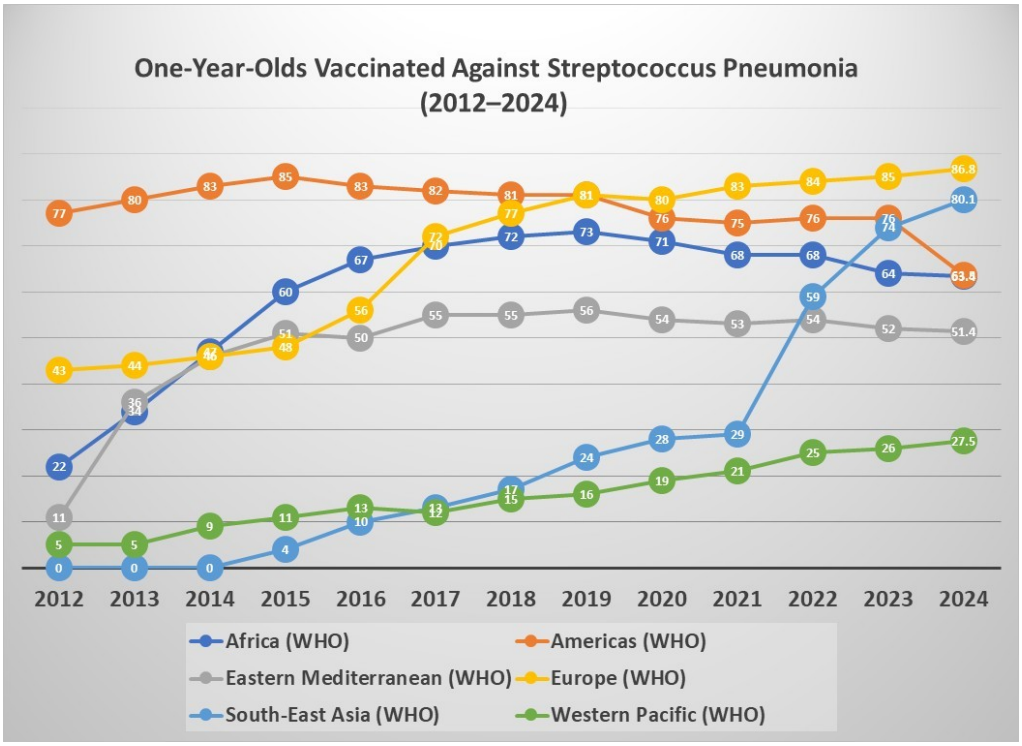


Figure 1: Yearly percentage of one-year-olds vaccinated against Streptococcus pneumoniae in different WHO regions from 2012 to 2024.

According to the World Health Organization, around 800,000 children under 5 years of age died in 2017, which represents 15% of all deaths in that age group. About 450 million people globally are affected by pneumonia each year, which is 7% of the world population. In Sub-Saharan Africa, pneumonia is the main cause of death in children under 5 years. It comprised 16% of all deaths, which is deadlier than malaria. According to Sara Mahtab and Dianna M. Balu, pneumonia contributed to 40.6% of deaths of all children in Africa and South Asia from 2016 to 2022. In America, more than 50,000 deaths are reported annually because of this lung infection; it is the most common cause of death in developing countries. In the United States, it ranks as the 8th leading cause of death. In 2016, around 31,540 people died in the European Union from pneumonia. The overall annual incidence of CAP in adults increases with age; men have a higher chance of getting infected than women. In the WHO Western Pacific region, 14% of all under 5 years mortality is due to pneumonia. More than 75% of pneumonia-related deaths occur in China and Cambodia. The Southeast Asia region experiences a

high risk of pneumonia, especially in children. India, in particular, has a high rate, with 43 million new cases annually and an estimated 3 million annual deaths. Pakistan is the third country that carries the greatest burden of child deaths, with approximately 90,398 deaths from pneumonia and diarrhea in 2020. Also, Table 1 [3, 5] illustrates the global pneumonia death cases from 2012 through 2024 for three age groups (under 5 years, 5–64 years, and above 64 years). In terms of mortality, this table indicates a clear decreasing trend among children under 5 years, while individuals above 64 years consistently accounts for the largest number of deaths. Overall, in recent years, a gradual decline has been observed in total pneumonia-related deaths; however, the number remains high and requires immediate efforts to reduce the spread. Figure 1 illustrates the yearly percentage of one-year-olds vaccinated against *Streptococcus pneumoniae*, as reported by the WHO in different regions from 2012–2024 [3, 5, 6]. This information represents an overall increasing trend in vaccination coverage in most regions, maintaining relatively higher and stable coverage levels in Europe and the Americas. However, the Western Pacific and South-East Asia regions show gradual improvement over time, whereas Africa shows a sharp rise in recent years.

In Bangladesh, diarrhea was the leading cause of child death in the past, but now pneumonia is the leading cause of child mortality. Pneumonia kills 24,000 children in Bangladesh every year, according to icddr,b (International Centre for Diarrhoeal Diseases Research, Bangladesh). Though mortality has reduced over the decades, the past 5 years have shown stagnation at about 7.4 deaths per thousand live births, 4 million new cases, and approximately 677,000 hospitalizations each year. A study by icddr,b from 2019 to 2021 showed that unique cases of pneumonia had a high occurrence of antibiotic-resistant Gram-negative bacteria. Furthermore, research conducted by icddr,b showed that vaccines, including RSV for pregnant women, help prevent severe pneumonia in infants. Moreover, Figure 2 illustrates the impact of pneumonia across three age groups in Bangladesh by including death cases between 2012 and 2024 [7]. This figure confirms that a steady decline over time is observed in deaths among children under 5 years, while a relatively stable situation with slight fluctuations occurs in the 5–64 years age group. However, a consistently increasing trend is observed in deaths among people above 64 years, eventually becoming the largest among all groups in later years.

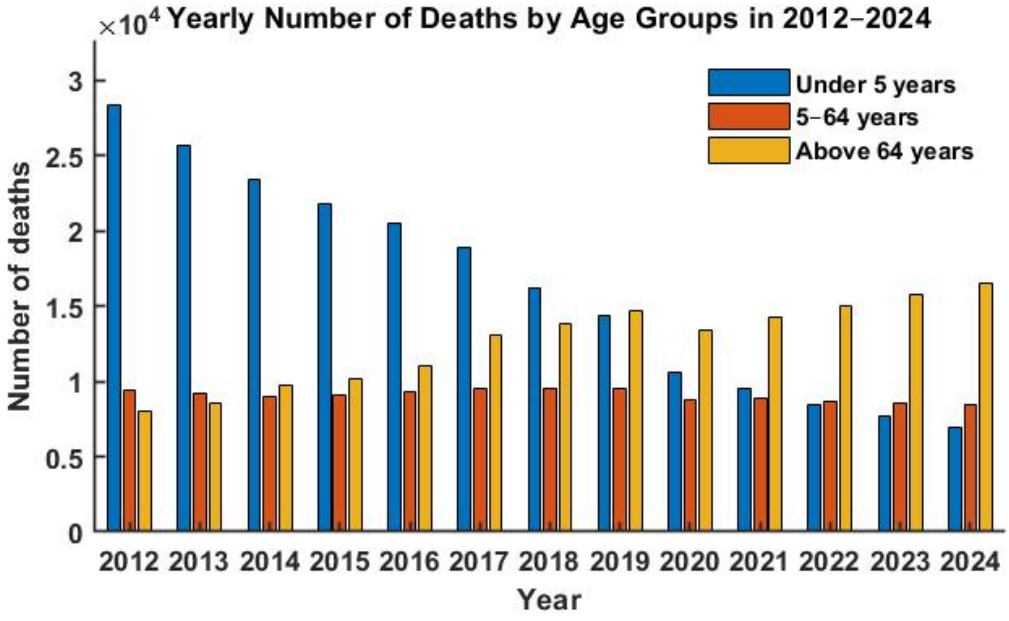


Figure 2: Yearly Number of deaths of people by different age groups, between 2012 and 2024 in Bangladesh.

Pneumonia may develop resistance to multiple antibiotics due to exposure, especially in children, and careful use of these is crucial to prevent resistance [8]. It kills over a million children each year in low-resource regions. Kosasih and Abeyratne used a wavelet-based crackling detection method to diagnose bacterial pneumonia quickly in children by analyzing a mathematical model of cough sounds [9]. It is a lung infectious disease that may be controlled by good vaccination, effective treatment, and reducing environmental risks [10].

Vaccination is recognized as one of the most effective approaches for preventing pneumonia and limiting its spread. Immunization against major pathogens, especially pneumococcal bacteria and influenza viruses, has contributed to reducing infection rates and mortality in many areas. Alongside vaccination, practices such as maintaining good hygiene, ensuring adequate nutrition, and obtaining early medical care help strengthen immunity and reduce the severity of illness. However, the impact of vaccination programs is not uniform across different age groups and regions, mainly due to variations in coverage, access, and public awareness. Moreover, in settings with limited resources, behavioral and environmental conditions may further reduce the effectiveness of vaccination efforts. Therefore, it is necessary to study vaccination alongside other preventive measures within a combined framework to better understand their overall influence on disease spread.

Despite significant work on pneumonia, several key challenges still exist. Many existing mathematical models assume a homogeneous population and do not account for age-specific differences, which are important for understanding disease dynamics, especially among children and older adults. Additionally, some models use age-specific compartments but do not include a vaccination compartment for different age groups. Although some models consider vaccination, they mainly study its effects within a single framework and do not develop optimal control models. Furthermore, only a few studies include medical interventions such as treatment and vaccination as control variables, but they often overlook practical factors like hygiene and nutrition, which are particularly important in developing countries. The use of optimal control approaches that integrate these factors is also limited, and comparisons between different intervention strategies are often not detailed enough to effectively guide policy decisions. These gaps highlight the need for more detailed models that include realistic assumptions, classify the population into three age groups (under 5 years, 5–64 years, and above 64 years), and incorporate vaccinated compartments for each age group, as well as consider additional control strategies beyond treatment and vaccination.

To address these limitations, this study proposes an age-structured mathematical model for pneumonia transmission that incorporates vaccination across three different age groups. The model is further extended through an optimal control framework by adding two practical strategies: balanced diet and hygiene practices. The basic reproduction number is calculated using the next-generation matrix approach, and both disease free and endemic equilibrium states are examined. The local and global stability of the system are analyzed, and sensitivity analysis is carried out to determine the most influential parameters. Numerical simulations are also performed to compare different control strategies, assess the role of vaccination, and show graphically how the parameters vary. In addition, a comparative cost-effectiveness analysis of the control strategies is conducted. The results provide a clear understanding of pneumonia transmission and offer a more practical basis for developing effective and informed control policies.

2 Literature Review

Recently, pneumonia has emerged as one of the most significant respiratory infectious diseases, exerting a substantial impact on global morbidity and mortality across all age groups. It poses a serious challenge to public health systems worldwide due to its rapid transmission and severe health consequences. The transmission dynamics of this disease are complex and strongly influenced by environmental, biological, and behavioral factors. Pneumonia can lead to serious health complications, increased hospitalization rates, and high mortality, particularly among high-risk populations. Therefore, it is crucial to better understand the spread of this disease and to develop effective control measures to reduce its transmission. Mathematical modeling, along with literature-based studies, plays a vital role in understanding the transmission of pneumonia and in developing effective control measures.

Pneumonia is an infectious disease that kills more children than other diseases such as AIDS, malaria, and measles, especially children under 5 years [11]. Mathematical modeling is widely used to understand

the transmission dynamics of pneumonia by using compartmental models and analyzing the stability of equilibrium points. It has already been shown that treatment and natural immunity play important roles in reducing disease prevalence and influencing the long-term dynamics of the disease. Most models use the basic reproduction number to determine threshold conditions and apply Lyapunov functions to study stability. Based on this idea, the authors in [12] studied the effect of treatment on pneumonia transmission and its impact on equilibrium stability and disease control. Additionally, Streptococcus pneumoniae is commonly found in the throat of young children and is responsible for causing diseases such as pneumonia and meningitis. Although a vaccine was introduced in 2000 that helps prevent some types of the disease and reduce its spread, a problem still remains, as the same genetic types can appear in different serotypes. To investigate and understand this issue, a basic differential equation model was used in [13] to study the relationship between sequence types and serotypes. The study evaluated the effective reproduction number, analyzed equilibrium and stability, and used simulations to examine how the disease spreads under different conditions.

In low-income countries with limited access to diagnosis, pneumonia is becoming one of the most severe causes of death among children under 5 years of age. An easy criterion for pneumonia diagnosis was introduced by the World Health Organization (WHO), focusing on high sensitivity and using easily measurable clinical signs. To improve the WHO pneumonia diagnosis criterion, the study [14] used 17 commonly measured clinical features and established a logistic regression-based method. Though the introduced method achieved similar sensitivity, it presented much higher specificity than the WHO criterion. The diagnosis of pneumonia can be improved through the mathematical analysis of routine clinical measurements and can be simply implemented on mobile phones, which is more useful in areas with limited medical resources. In the same year, another study [15] developed a nonlinear mathematical model in a population whose size changes over time. This study evaluated the effective reproduction number and checked the stability of the disease-free and endemic equilibria. Bifurcation and sensitivity analysis of the basic reproduction number were conducted to identify key parameters. Additionally, Pontryagin's Maximum Principle was used to identify the best control strategy among three considered strategies, namely education, treatment, and screening. This study confirmed that the most cost-effective control measure was the combination of prevention and treatment. In the next year, a transmission and control model of bacterial pneumonia caused by Streptococcus pneumoniae was introduced with two control measures, treatment and vaccination. Then, in [16], the authors performed various mathematical analyses, evaluated the disease-free and endemic equilibria, analyzed their stability, and calculated the basic reproduction number. They proved that if $R_0 < 1$, then the disease-free equilibrium is stable, while for $R_0 > 1$, the endemic equilibrium is globally stable. They also showed that combining treatment and vaccination interventions can potentially eradicate this infection, which was also supported by numerical simulations.

Mathematical modeling (deterministic and stochastic models) serves as an important tool for understanding the transmission of infectious diseases. The authors in [17] worked with stochastic models, which provided a probabilistic framework for describing the uncertainty and variability in disease transmission. They also analyzed various deterministic models to provide a basic idea for constructing stochastic models for further research. After that, in [18], a multi-level mathematical model was developed to investigate Streptococcus pneumoniae pneumonia and the effects of antibiotic treatment timing. This study showed that the inflammatory response can be reduced by early antibiotic treatment, especially for elderly people. The insights obtained from this work suggest that early or prophylactic antibiotic treatment is helpful for reducing the severity of pneumonia in hospitalized elderly individuals. Furthermore, to study the dynamics of Streptococcus pneumoniae transmission, a study [19] considered an SVEIR model with vaccination to show that sufficient vaccination coverage can eliminate this disease. This work also emphasized the importance of the capacity and efficacy of treatment strategies in controlling pneumonia transmission. At the same time, another study [20] considered vaccination, symptomatic carriers, and asymptomatic carriers to develop a mathematical model and investigated the spread and control of bacterial pneumonia. This study showed that reducing and eradicating this infection in the long term can be possible with the help of effective vaccination. Another work showed that not only treatment but also natural immunity can affect the spread of this infection [21]. Next, in [22], the authors introduced a deterministic mathematical model to demonstrate the transmission of pneumonia–HIV co-infection and developed a control model with two control measures: anti-pneumonia and ART treatments. They applied Pontryagin's Maximum Principle to identify the most effective control strategy for such co-infection. Moreover, a delayed mathematical model incorporating susceptible,

carrier, infected, and recovered compartments was used to understand the transmission of pneumonia among children in [23]. Different mathematical analyses were conducted in this study, supported by numerical simulations. Incidence data from five districts in Jakarta, Indonesia, were used and a mathematical model was established in [24] to show the effects of vaccination on the transmission of pneumonia. The authors proved that $R_0 < 1$ can eliminate this disease without any backward bifurcation. They also demonstrated the effectiveness of vaccination for adults, while combining adult and newborn vaccination ensures better long-lasting immunity. Under various vaccination strategies, a mathematical model was developed to examine invasive pneumococcal disease (IPD) and pneumococcal carriage in Germany. The findings of this study showed that the disease burden among older patients increased due to non-PCV13 serotypes, whereas PCV15 was predicted to show lower protection than PCV20 against pneumococcal disease in [25].

Additionally, in 2024, a study considered a fractional-order SVEIR model for understanding pneumonia transmission using the Caputo fractional derivative. The authors of [26] proved that if vaccination coverage exceeds the critical threshold, then pneumonia can be eradicated. Also, they found two highly sensitive parameters: the transmission and progression rates. In the same year, Shyamsunder and Purohit used a deterministic SVEIR model with Caputo fractional derivatives to study how pneumonia spreads. They explained the effective impact of vaccination coverage and treatment in reducing transmission and controlling the spread of this infection. Chukwu, Tchoumi, and Diagne developed a mathematical model to analyze pneumonia dynamics in high-risk populations, particularly children under 5 years and adults over 65. The sensitivity analysis identified key parameters influencing infection spread, highlighting the importance of early treatment in controlling disease transmission. The basic reproduction number for this model was $R_0 = 1.157$, which indicated that the pneumonia disease in this region was epidemic [27].

Globally, pneumonia is the leading infectious cause of mortality for children. In 2019, pneumonia killed 740180 children under the age of five, making up 22% of all fatalities in children aged 1 to 5 and 14% of all deaths in children under the age of five. More than 2,000,000 children die from pneumonia, the worst sickness, especially those under the age of five and those over 65. In underdeveloped nations like Asia, Africa, and Europe, pneumonia is a dreadful burden. Developed nations have implemented the pneumococcal vaccine, and for sinister reasons, the United States is the biggest contributor. A broader type of deterministic modeling is called delay modeling. A more practical, intimate, and genuine method of managing infectious illnesses is delayed analysis [28]. Based on above findings, now it's high time to be inspired to do a study in this field. In [27], the authors developed a model for three different age groups but they did not include vaccination compartments for respective age groups and provide any description regarding the effects of vaccination across three different age groups as well as other interventions with the presence of vaccination. Therefore, we introduce a pneumonia transmission model based on three age groups with vaccination compartment and a control model involving two invention variables with the presence of vaccination–balanced diet and hygiene–reduce the transmission and control the spread of this disease.

The present study provides several new developments in mathematical epidemiology, focusing on pneumonia transmission. At first, a vaccinated population compartment is implemented to realistically represent pneumococcal immunization across different age groups. Secondly, global sensitivity analysis using the LHS-PRCC method is employed to analyze the effective parameters impacting the basic reproduction number (R_0), along with control planning. Thirdly, balanced diet and hygiene are incorporated within an optimal control framework to minimize transmission and manage pneumonia disease spread. The findings provide important insights for both theoretical studies and public health planning, improving the reduction of pneumonia transmission based on published evidence and available data, with additional parameters estimated using biologically reasonable assumptions. The paper is organized as follows.:

A prior version (A.1) of the proposed model (3.1) is included in Appendix A, whereas the extended disease spread framework (3.1) is formulated in Section 3.1. In Section 3.3, the parameter values are introduced and applied in the extended pneumonia spread framework (3.1). Appendix B examines the well-posedness, non-negativity, and boundedness of the proposed model (3.1); evaluates both the disease-free and endemic equilibrium points; analyzes the local and global stability of both the disease-free equilibrium and the endemic equilibrium; demonstrates the procedure for deriving the basic reproduction number R_0, computes its numerical value, and provides its biological interpretation in Section 3.2.2, along with a global sensitivity analysis to identify the most influential parameters in Section

4.1. The optimal control framework (3.4) incorporating two control factors—balanced diet (B_c, B_m, B_a) and hygiene (H_c, H_m, H_a)—is then explained in Section 3.4, followed by its characterization using Pontryagin's Maximum Principle in Sections 3.4.1–3.4.2. Later, a comparative study between the baseline model (A.1) without vaccination and the proposed model (3.1) with vaccination for three different age groups is included in Section 4.2, using the Runge-Kutta fourth-order method within MATLAB for numerical simulation and graphical demonstration. Additionally, Section 4.3 describes how different parameters affect pneumonia transmission, whereas the optimal control model (3.4) with three distinct cases, only balanced diet, only hygiene, and both balanced diet and hygiene, illustrates how different control variables affect the disease in Section 4.4. Moreover, Section 4.4.1 presents a comparative study of the cost-effectiveness of the two control strategies. The study is finally concluded with important findings and comments in Section 5.

3 Methodology

3.1 Model Formulation

In this section, by taking into account a closed population that consists of three subgroups of persons at high risk of infection, we create a subgroup population dynamics model of pneumonia infection. These three subgroups are divided into three categories: adults above 64 years, people between the ages of 5–64 years, and children under 5 years. Consequently, our model has 14 compartments, where the susceptible population is divided into three age groups: above 64 years (S_a), 5–64 years (S_m), and under 5 years (S_c). Similarly, the exposed population considers three age groups: E_a, E_m, and E_c, while the infectious population is classified into three types: I_a, I_m, and I_c. Additionally, this model includes a treated population (T) and a recovered population (R). Further, a new class "vaccination" is added to the modified pneumonia transmission model, where the vaccinated population is categorized as above 64 years (V_a), 5–64 years (V_m), and under 5 years (V_c).

Table 2: Biological meanings of state variables.

S_a	Susceptible population over 64
S_m	Susceptible population between 5 and 64
S_c	Susceptible population under 5
E_a	Exposed population over 64
E_m	Exposed population between 5 and 64
E_c	Exposed population under 5
I_a	Infectious population over 64
I_m	Infectious population between 5 and 64
I_c	Infectious population under 5
T	Treated population
R	Recovered population
V_a	Vaccinated individuals over 64
V_m	Vaccinated individuals between 5 and 64
V_c	Vaccinated individuals under 5

The Tables 2 and 3 summarize the state variables and model parameters, respectively. Tables 2 stands for the biological meanings of all state variables, which are categorized into susceptible, exposed, infectious, treated, recovered, and vaccinated classes across three age groups: under 5 years, 5–64 years, and above 64 years. Table 3 summarizes the model parameters, including contact rates, recovery and treatment rates, mortality rates, vaccination rates, progression rates, and other epidemiological factors that govern the dynamics of pneumonia transmission within the population. Moreover, to understand the pneumonia transmission dynamics properly, here we introduce the pictorial representation (Figure 3) of the pneumonia transmission framework (3.1) including vaccination classes for three different age groups.

Figure 3 displays the schematic representation of the proposed pneumonia transmission model (3.1) with vaccination for three distinct age groups: under 5 years (c), 5-64 years (m), and above 64 years (a). The structure of this model (3.1) demonstrates the population flow through different epidemiological compartments, capturing disease progression. However, maturation rates δ_{cm} and δ_{ma} are only considered for the susceptible population for simplicity. Initially, individuals enter the susceptible classes

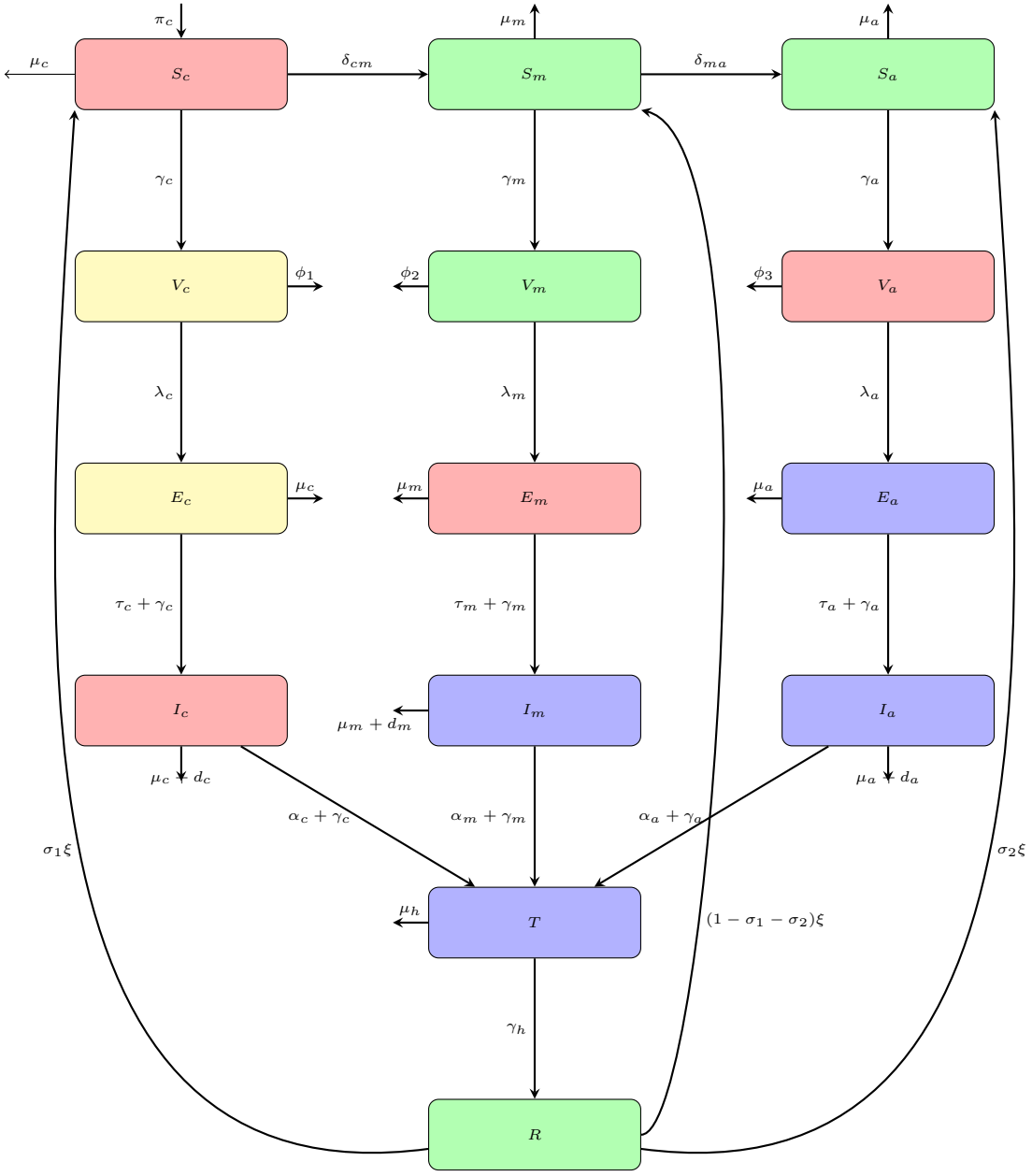


Figure 3: Pictorial representation of Pneumonia Transmission Model with Vaccination for Three Different Age Groups.

Table 3: Biological meanings of parameters.

$\beta_c, \beta_m, \beta_a$	Contact rates for I_c, I_m, I_a
γ_h	Recovery rate
$\alpha_c, \alpha_m, \alpha_a$	Treatment rates
d_c, d_m, d_a	Death rates for I_c, I_m, I_a
σ_1, σ_2	Proportion of recovered who become S_a, S_c
μ_h	Natural mortality rate of humans
μ_c, μ_m, μ_a	Natural death rates
η	Modification parameter for I_m
ξ	Rate of loss of immunity
τ_c, τ_m, τ_a	Progression rates for I_c, I_m, I_a
Π_c	Recruitment rate for newborns into S_c
δ_{cm}	Maturation rate for S_c to S_m
δ_{ma}	Maturation rate for S_m to S_a
$\gamma_c, \gamma_m, \gamma_a$	Rate at which susceptible individuals get vaccinated
$\lambda_c, \lambda_m, \lambda_a$	Force of infection rates

S_c, S_m, and S_a, where there is a possibility of acquiring infection through contact with infected individuals, or moving to the vaccinated classes V_c, V_m, and V_a through vaccination programs. These vaccinated populations are considered to have reduced susceptibility. In contrast, partial protection or waning immunity may allow transition back to the susceptible or exposed classes. After that, the population moves to the exposed classes E_c, E_m, and E_a, where they are infected but not yet able to spread the infection. They enter the infected classes I_c, I_m, and I_a after the incubation period and then start to transmit the infection to others. Next, they may receive treatment and move to the treatment class T, then move to the recovery class depending on their condition. This class T reduces the infection and supports recovery. The recovered compartment R contains those who receive temporary immunity after treatment. However, there is a possibility that immunity decreases over time, so they may return to the susceptible class and become infected again. This model (3.1) also includes natural death (μ_i), disease-related death (d_i), and progression (τ_i), which are indicated by arrows between compartments. Overall, Figure 3 represents how different age groups are connected in the process of pneumonia transmission.

There exist several pneumococcal vaccines that differ in terms of target age groups, spectrum of protection against pneumococcal serotypes, vaccine formulation, and effectiveness among different risk populations. From the perspective of the World Health Organization (WHO), pneumococcal conjugate vaccines (PCVs) are recommended globally and are included in childhood immunization programs in most countries. For instance, currently licensed pneumococcal vaccines include pneumococcal conjugate vaccines such as PCV13, PCV15, and PCV20, as well as the pneumococcal polysaccharide vaccine PPSV23, which are used for adults ≥ 50 with different clinical indications [29]. In most studies, authors assume a uniform vaccine or focus only on high-risk individuals. Nevertheless, this study does not focus on any particular pneumonia vaccine. Instead, a generalized vaccination framework is incorporated into the model, characterized by age-specific vaccination rates and moderate vaccine effectiveness with three age groups: over 64, aged 5–64, and under 5, to evaluate the overall impact of vaccination on pneumonia transmission. Consequently, the proposed model remains reliable and applicable across a wide range of epidemiological scenarios in which effective pneumonia vaccines are implemented, regardless of the specific vaccine formulation used.

We made the following assumptions [24, 27] in order to propose our modified pneumonia transmission model (3.1):

1. The total human population is classified into three age groups: under 5 years, 5–64 years, and above 64 years. Although four epidemiological compartments (S, E, I, V) are age-structured, transitions between age classes (at rates δ_{cm} and δ_{ma}) are taken to occur only within the susceptible population for keeping the model simple and consistent with the baseline framework. For the same reason, the treatment and recovered compartments (T, R) are considered as aggregated classes and are not stratified by age.

2. Individuals can mix homogeneously within three age groups and the force of infection $(\lambda_i, i = c, m, a)$ varies across age classes.

3. Susceptible populations of all groups transform to exposed due to infection, while the exposed individuals tend to infectious with the age-specific progress rates (τ_c, τ_m, τ_a). Then, the infected

population recover or die out due to infection.

4. After getting treatment population can move to the recovered population at a certain recovery rate (γ_h) and sometimes the recovered population can partially lose immunity and back to susceptible population.
5. Vaccinated population is allowed as age-specific: V_c under 5 years, V_m between 5-64 years, and V_a above 64 years, with the rates $\gamma_c, \gamma_m, \gamma_a$ respectively. Additionally, vaccination have partial immunity with the efficacy failure rate ξ. Moreover, a significant number of children who are at risk and a few number of other aged people, get the vaccine (based on real-world data or an estimated coverage rate).
6. Recruitment rate is considered only for susceptible population, S_c, under 5 years at a rate Π_c.
7. Age-specific natural death rates are μ_c, μ_m, μ_a, while d_c, d_m, d_a are the death rates due to infection.
8. There is no variation of season over the transmission; vaccination and treatment are assumed as constants and do not depend on any behavior.
9. Individuals transition immediately to the vaccinated class. Vaccination can be given all at once (routine) or at set times (campaign).
10. People don't get booster shots (unless they are specifically depicted). People get vaccinated at a steady pace, like a certain number of people every day.
11. All targeted people who are eligible will eventually get vaccinated if there is enough coverage.

Considering all the assumptions, we have defined the following Pneumonia transmission model with vaccination:

$$\begin{cases} S_c' &= \Pi_c + \sigma_1\xi R - (\mu_c + \delta_{cm} + \lambda_c + \gamma_c)S_c, \\ S_m' &= \delta_{cm}S_c(1-\sigma_1-\sigma_2)\xi R - (\mu_m + \delta_{ma} + \lambda_m + \gamma_m)S_m, \\ S_a' &= \delta_{ma}S_m + \sigma_2\xi R - (\mu_a + \lambda_a + \gamma_a)S_a, \\ E_c' &= \lambda_c S_c - (\mu_c + \tau_c + \gamma_c)E_c, \\ E_m' &= \lambda_m S_m - (\mu_m + \tau_m + \gamma_m)E_m, \\ E_a' &= \lambda_a S_a - (\mu_a + \tau_a + \gamma_a)E_a, \\ I_c' &= \tau_c E_c - (\mu_c + d_c + \alpha_c + \gamma_c)I_c, \\ I_m' &= \tau_m E_m - (\mu_m + d_m + \alpha_m + \gamma_m)I_m, \\ I_a' &= \tau_a E_a - (\mu_a + d_a + \alpha_a + \gamma_a)I_a, \\ T' &= \alpha_c I_c + \alpha_m I_m + \alpha_a I_a - (\mu_h + \gamma_h)T, \\ R' &= \gamma_h T - (\mu_h + \phi)R, \\ V_c' &= \gamma_c S_c - \lambda_c V_c + \phi_1 R, \\ V_m' &= \gamma_m S_m - \lambda_m V_m + \phi_2 R, \\ V_a' &= \gamma_a S_a - \lambda_a V_a + \phi_3 R, \end{cases} \tag{3.1}$$

with positive initial conditions,

$$\begin{cases} S_c(0) \geq 0, S_m(0) \geq 0, S_a(0) \geq 0, E_c(0) \geq 0, E_m(0) \geq 0, E_a(0) \geq 0, I_c(0) \geq 0, \\ I_m(0) \geq 0, I_a(0) \geq 0, T(0) \geq 0, R(0) \geq 0, V_c(0) \geq 0, V_m(0) \geq 0, V_a(0) \geq 0. \end{cases} \tag{3.2}$$

The model (3.1) will be biologically meaningful, if the variables are non-negative. That is, due to the positive initial conditions, the obtained outcome from proposed model (3.1) remains non-negative. In

this model, all the variables (3.1) have non-negative numbers, so it has ecological importance. It means that due to the positive initial conditions, the outcome of the study (3.1) remains non-negative for time $t \geq 0$. In this specific pneumonia transmission framework (3.1), the invariant regions are shown. Here, the susceptible, exposed, and infectious compartments are structured according to three age groups, namely children under 5 years, individuals aged 5–64 years, and adults above 64 years. However, following the structure of the reference model (A.1) [27], the treated and recovered compartments are considered as single aggregated classes and are not stratified by age. This assumption is adopted to maintain consistency with the original framework (A.1) [27] and to avoid increasing model complexity. Recovered individuals lose immunity at rate ξ and return to the susceptible classes. The parameters σ_1 and σ_2 determine the redistribution of these individuals into different age groups, which reflects age-dependent reinfection dynamics. Vaccinated individuals may still become infected through the force of infection terms $\lambda_c V_c$, $\lambda_m V_m$, and $\lambda_a V_a$, representing imperfect vaccine protection in each age group.

The key mathematical distinction between the previous mathematical framework (A.1) and the our developed framework (3.1) lies in the introduction of vaccinated class to three different age groups. This modification increases the dimension of the model and affects disease spread. In contrast to the previous framework and the developed framework (3.1) permits movement from susceptible into vaccinated state, which successfully decrease the infected numbers. Similar matters have been discussed in [16], where they described the vaccination effects only for one susceptible population in general. But in this study, the authors combine the idea of both [16] and [27], and propose a new mathematical model (3.1). In which, the model (3.1) is concerned to the modification of vaccination for three different age groups for susceptible population: children under 5 years, 5–64 years, and above 64 years. This enhancement is captured in the developed mathematical framework of differential equations and updated force of infection, which eliminates vaccinated people. Basic reproduction number, R_0 [33], is recalculated using the next-generation matrix approach because of the addition of new parameters: vaccination rate for three individual populations (γ_c, γ_m, γ_a) and vaccination rate for treated individuals (ϕ_1, ϕ_2, ϕ_3). This revised R_0 aids in assessing the relationship between vaccination efficacy and coverage and the risk of disease transmission. The updated model now includes structural changes to reflect vaccination evolution as well as improve the study's suitability for assessing epidemiology. The correct specification and calculation of numerous epidemiological and biological characteristics are critical to the accuracy and use of our pneumonia transmission model. In addition to helping characterize the interactions among vulnerable individuals, infected individuals, and other pertinent population groups, these criteria simplify the complex nature of pneumonia dissemination.

3.2 Mathematical analysis

3.2.1 Equilibrium Points

The disease-free and endemic equilibrium points of the model (3.1) are presented below, while their detailed calculations are provided in Appendix B (Sections B.1 and B.2).

$$\begin{cases} E_0 = \left(S_c^0, S_m^0, S_a^0, 0, 0, 0, 0, 0, 0, 0, 0, V_c^0, V_m^0, V_a^0\right); \\ S_c^0 = \frac{\Pi_c}{(\mu_c+\delta_{cm}+\gamma_c)}, S_m^0 = \frac{\Pi_c\delta_{cm}}{(\mu_c+\delta_{cm}+\gamma_c)(\mu_m+\delta_{ma}+\gamma_m)}, \\ S_a^0 = \frac{\Pi_c\delta_{cm}\delta_{ma}}{(\mu_a+\gamma_a)(\mu_c+\delta_{cm}+\gamma_c)(\mu_m+\delta_{ma}+\gamma_m)}, V_c^0 = \frac{\Pi_c\gamma_c}{\mu_c(\mu_c+\delta_{cm}+\gamma_c)}, \\ V_m^0 = \frac{\Pi_c\delta_m\gamma_m}{\mu_m(\mu_c+\delta_{cm}+\gamma_c)(\mu_m+\delta_{ma}+\gamma_m)}, V_a^0 = \frac{\Pi_c\delta_{cm}\delta_{ma}\gamma_a}{\mu_a(\mu_a+\gamma_a)(\mu_c+\delta_{cm}+\gamma_c)(\mu_m+\delta_{ma}+\gamma_m)}, \end{cases}$$

and

$$\begin{cases} E_i^{**} = \frac{\lambda_i S_i^{**}}{\mu_i+\tau_i+\gamma_i}, I_i^{**} = \frac{\tau_i\lambda_i S_i^{**}}{(\mu_i+\tau_i+\gamma_i)(\mu_i+d_i+\alpha_i+\gamma_i)}, \\ T^{**} = \frac{\sum_{i=c}^{m}\alpha_i I_i^{**}}{\mu_h+\gamma_h}, R^{**} = \frac{\gamma_h\sum_{i=c}^{m}\alpha_i I_i^{**}}{(\mu_h+\phi)(\mu_h+\gamma_h)}, V_i^{**} = \frac{\gamma_i S_i^{**}+\phi_1 R^{**}}{\lambda_i}, i = c, a, m, \\ S_c^{**} = \frac{\Pi_c+\sigma_1\xi R^*}{\mu_c+\delta_{cm}+\lambda_c+\gamma_c}, S_m^{**} = \frac{\delta_{cm}S_c^{**}(1-\sigma_1-\sigma_2)\xi R^*}{\mu_m+\delta_{ma}+\lambda_m+\gamma_m}, S_a^{**} = \frac{\delta_{ma}S_m^{**}+\sigma_2\xi R^*}{\mu_a+\lambda_a+\gamma_a}. \end{cases}$$

3.2.2 Biological Interpretation of R_0

The basic reproduction number is

$$R_0 = R_c + R_m + R_a = \frac{\beta_c \tau_c A_1}{g_1 g_4} + \frac{\beta_m \tau_m A_2}{g_2 g_5} + \frac{\beta_a \tau_a A_3}{g_3 g_6}. \tag{3.3}$$

This expression is derived using the next-generation matrix method, and the detailed calculations are provided in Appendix B (Section B.3). In equation (3.3), the formulation of R_0 includes significant parameters, as explained in the following section:

- $\beta_c, \beta_m, \beta_a$ represents the effective contact rates of infectious individuals in the child, middle-aged, and elderly populations, respectively. Higher values of these parameters increase the value of R_0.
- τ_c, τ_m, τ_a denote the progression rates from the exposed to the infectious classes for the respective age groups. A growth in these parameters causes a corresponding growth in R_0.
- $\alpha_c, \alpha_m, \alpha_a$ represents the treatment rates of infectious individuals in each group. Higher treatment rates decrease the value of R_0.
- d_c, d_m, d_a and μ_c, μ_m, μ_a are the disease-induced and natural mortality rates, respectively. An increase in these parameters shortens the infectious period and consequently reduces R_0.
- All remaining parameters have an inverse relationship with R_0.

3.2.3 Stability Results

In this part, we present a concise summary of the results concerning the well-posedness of the system, and the stability analysis, including both local and global cases. The fundamental theory of dynamical systems applied to the model (3.1) establishes the well-posedness of the system, including the existence of an invariant region, positivity, and boundedness of solutions, as rigorously shown in Lemma B.1 of the Appendix. B. The model (3.1) provides a unique disease-free equilibrium (DFE) E_0 and a unique endemic equilibrium E_1 if $R_0 > 1$. The basic reproduction number R_0 works as a threshold parameter controlling the disease dynamics. Specifically, when $R_0 < 1$, the DFE E_0 is locally asymptotically stable, while it becomes unstable for $R_0 > 1$, leading to the existence of a unique endemic equilibrium E_1, as proved in Theorem B.2, Appendix B. Furthermore, the global dynamics show that if $R_0 < 1$, the disease-free equilibrium E_0 is globally asymptotically stable, while if $R_0 > 1$, the endemic equilibrium E_1 is globally asymptotically stable. Thus, R_0 helps to determine the long-term behavior of the system, ensuring disease extinction or persistence. The detailed proof is provided in Appendix B (Theorem B.4).

3.3 Parameter Values

In this subsection, we will describe the values of the parameters used in the comprehensive modeling of pneumonia transmission. We have taken the values of some parameters from the suggested paper [27]. Contact rates for I_c, I_m, I_a denoted by β_c, β_m, and β_a respectively. Treatment rates are denoted by α_c α_m, α_a respectively. Death rates for I_c, I_m, I_a are denoted by d_c, d_m, d_a respectively. Progression rates for I_c, I_m, I_a are denoted by τ_c, τ_m, τ_a respectively. Natural death rates are denoted by μ_c, μ_m, μ_a respectively. η is the modification parameter for I_m, and γ_c, γ_m, γ_a are the rates at which susceptible individuals get vaccinated. The force of infection rates λ_i are defined as $\lambda_c = \frac{\beta_c(I_c+\eta I_m+I_a)}{N}$, $\lambda_m = \frac{\beta_m(I_c+\eta I_m+I_a)}{N}$, $\lambda_a = \frac{\beta_a(I_c+\eta I_m+I_a)}{N}$, N=total population [27]. The parameter values adopted from [27], along with newly introduced parameters based on literature-supported assumptions, are presented in Table 4.

Table 4: Parameter values adopted from [27] and other relevant literature-based assumptions for the updated model (3.1).

Parameters	Range	Value	Unit	Reference
β_c		0.1267	day^{-1}	[27]
β_m		0.1028	day^{-1}	[27]
β_a		0.1379	day^{-1}	[27]
τ_c	[0.167, 0.25]	0.2	day^{-1}	[27]
τ_m	(0, 1)	0.5	day^{-1}	[27]
τ_a	(0, 1)	0.590313	day^{-1}	[27]
α_c	[0.0357, 0.142857]	0.0476	day^{-1}	[27]
α_m	(0, 1)	0.03	day^{-1}	[27]
α_a	(0, 1)	0.025	day^{-1}	[27]
η	(0, 1)	0.895	unitless	[27]
d_c	(0.00121, 0.00363)	0.00360	day^{-1}	[27]
d_m	(0.001, 0.002)	0.002	day^{-1}	[27]
d_a	(0, 1)	0.00264	day^{-1}	[27]
δ_{cm}		5.47945×10^{-4}	day^{-1}	[27]
δ_{ma}		4.72367×10^{-5}	day^{-1}	[27]
Π_c	(1, 10687)	100	day^{-1}	[27]
μ_c		1.479×10^{-5}	day^{-1}	[27]
μ_m	$(3.7, 18.26) \times 10^{-5}$	4.93×10^{-5}	day^{-1}	[27]
μ_a	$(10.9589, 19.569) \times 10^{-5}$	13.6986×10^{-5}	day^{-1}	[27]
μ_h		$\frac{1}{76.4\times365}$	day^{-1}	[27]
σ_1	(0, 1)	0.55	day^{-1}	[27]
σ_2	(0, 1)	0.35	day^{-1}	[27]
ϑ_{cm}		54.7945×10^{-5}	day^{-1}	[27]
ϑ_{ma}		4.72×10^{-5}	day^{-1}	[27]
γ_h	[0.0357, 0.0714]	0.0357	day^{-1}	[27]
ξ	(0, 1)	0.07	day^{-1}	[27]
γ_c	(0, 1)	0.814	day^{-1}	Literature-based assumption [16, 24, 26, 27, 28, 29]
γ_m	(0, 1)	0.03	day^{-1}	Literature-based assumption [16, 24, 26, 27, 28, 29]
γ_a	(0, 1)	0.23	day^{-1}	Literature-based assumption [16, 24, 26, 27, 28, 29]

The baseline parameters are adopted from an existing pneumonia transmission model [27], which does not include vaccination. In this study, vaccination is newly incorporated; therefore, vaccination-related parameters are not directly available from the original source. These parameters are based on values reported in published studies [16, 24, 26, 27, 28, 29] and are selected within epidemiologically realistic ranges, consistent with global vaccination trends reported by the World Health Organization.

3.4 Optimal Control Strategies

To have an appropriate control for our changed model (3.1) we will include two intervention strategies: balanced diet and hygiene with the factors B_c, B_m, B_a and H_c, H_m, H_a, respectively. The system of

differential equations describing the modified controlled model is written as,

$$\begin{cases} S_c' &= \Pi_c + \sigma_1(1-H_c)(1-B_c)\xi R - (\mu_c + \delta_{cm} + \lambda_c + \gamma_c)S_c, \\ S_m' &= \delta_{cm}S_c(1-\sigma_1-\sigma_2)(1-H_m)(1-B_m)\xi R - (\mu_m + \delta_{ma} + \lambda_m + \gamma_m)S_m, \\ S_a' &= \delta_{ma}S_m + \sigma_2(1-H_a)(1-B_a)\xi R - (\mu_a + \lambda_a + \gamma_a)S_a, \\ E_c' &= \lambda_c S_c(1-H_c)(1-B_c) - (\mu_c + \tau_c + \gamma_c)E_c, \\ E_m' &= \lambda_m S_m(1-H_m)(1-B_m) - (\mu_m + \tau_m + \gamma_m)E_m, \\ E_a' &= \lambda_a S_a(1-H_a)(1-B_a) - (\mu_a + \tau_a + \gamma_a)E_a, \\ I_c' &= \tau_c E_c - (\mu_c + d_c + \alpha_c + \gamma_c)I_c, \\ I_m' &= \tau_m E_m - (\mu_m + d_m + \alpha_m + \gamma_m)I_m, \\ I_a' &= \tau_a E_a - (\mu_a + d_a + \alpha_a + \gamma_a)I_a, \\ T' &= \alpha_c I_c + \alpha_m I_m + \alpha_a I_a - (\mu_h + \gamma_h)T, \\ R' &= \gamma_h T - (\mu_h + \phi)R, \\ V_c' &= \gamma_c S_c - \lambda_c V_c + \phi_1 R, \\ V_m' &= \gamma_m S_m - \lambda_m V_m + \phi_2 R, \\ V_a' &= \gamma_a S_a - \lambda_a V_a + \phi_3 R. \end{cases} \tag{3.4}$$

In this study, we have introduced a quadratic objective function in order to measure the control cost, where the costs of intervention are non-linear. This assumption relies on the fact that there is no linear relationship between the effects of the interventions and their associated costs on the infected populations. Consequently, quadratic cost functions have been commonly adopted in the literature.

$$J = \int_0^T (I_t + C_H H^2 + C_B B^2)dt.$$

The term C_H, C_B describe the cost of control efforts on minimizing hygiene and balanced diet respectively. Our aim is to find an optimal pair of B_i^* and H_i^*, such that

$$(B_i^*, H_i^*) = J_\Gamma min(B_i, H_i)$$

Here,

$$\Gamma = \{(B_i, H_i) \mid 0 \le B_i \le B_i^{\max}, 0 \le H_i \le H_i^{\max}\}, \text{where } i = c,\ m,\ a.$$

Applying Pontryagin's Maximum Principle [30, 31], Hamiltonian $\mathbf{H}$ is introduced, including state equations, objective functions and adjoint variables. That is,

$$\mathbf{H} = I_i(t) + C_{H_i}H_i^2 + C_{B_i}B_i^2 + \sum_{j=1}^{14}\lambda_j x_j,$$

where, $\lambda_j = \lambda_1, \lambda_2, \lambda_3, \lambda_4, \lambda_5, \cdots, \lambda_{14}$; $x_j = S_c, S_m, S_a, E_c, E_m, E_a, \cdots, V_c, V_m, V_a$.

According to Pontryagin's Maximum Principle, the adjoint variables satisfy

$$\lambda_j'(t) = -\frac{\partial \mathbf{H}}{\partial x_j}, \quad j = 1, 2, \ldots, 14,$$

with terminal conditions

$$\lambda_j(T_f) = 0.$$

Now, we derive each adjoint equation explicitly. Adjoint equation for λ_1 (associated with S_c):

From the controlled system (3.4), the dynamics of S_c are given by

$$S_c' = \Pi_c + \sigma_1(1-H_c)(1-B_c)\xi R - (\mu_c + \delta_{cm} + \lambda_c + \gamma_c)S_c.$$

Only terms involving S_c contribute to $\frac{\partial \mathbf{H}}{\partial S_c}$. We compute each contribution separately.

Contribution from S_c' term: $\lambda_1 S_c' = -\lambda_1(\mu_c + \delta_{cm} + \lambda_c + \gamma_c)S_c$. Hence, $\frac{\partial}{\partial S_c}(\lambda_1 S_c') = -\lambda_1(\mu_c + \delta_{cm} + \lambda_c + \gamma_c)$. Contribution from S_m' term: $S_m' = \delta_{cm}S_c(1-\sigma_1-\sigma_2)(1-H_m)(1-B_m)\xi R - (\mu_m + \delta_{ma} + \lambda_m + \gamma_m)S_m$, thus, $\frac{\partial}{\partial S_c}(\lambda_2 S_m') = \lambda_2\delta_{cm}(1-\sigma_1-\sigma_2)(1-H_m)(1-B_m)\xi R$.

Contribution from E_c' term: $E_c' = \lambda_c S_c(1-H_c)(1-B_c) - (\mu_c + \tau_c + \gamma_c)E_c$, such that $\frac{\partial}{\partial S_c}(\lambda_4 E_c') = \lambda_4\lambda_c(1-H_c)(1-B_c)$.

Contribution from V_c' term: $V_c' = \gamma_c S_c - \lambda_c V_c + \phi_1 R$, which yields, $\frac{\partial}{\partial S_c}(\lambda_{12} V_c') = \lambda_{12}\gamma_c$.

Combining all terms, we obtain:

$$\frac{\partial \mathbf{H}}{\partial S_c} = -\lambda_1(\mu_c + \delta_{cm} + \lambda_c + \gamma_c) + \lambda_2\delta_{cm}(1-\sigma_1-\sigma_2)(1-H_m)(1-B_m) + \lambda_4\lambda_c(1-H_c)(1-B_c) + \lambda_{12}\gamma_c.$$

Finally, applying $\lambda_1' = -\frac{\partial \mathbf{H}}{\partial S_c}$ yields

$$\lambda_1' = (\mu_c + \delta_{cm} + \lambda_c + \gamma_c)\lambda_1 - \lambda_2\delta_{cm}(1-\sigma_1-\sigma_2)(1-H_m)(1-B_m) - \lambda_4\lambda_c(1-H_c)(1-B_c) - \lambda_{12}\gamma_c.$$

Similarly, $\frac{\partial \mathbf{H}}{\partial S_m} = -\lambda_2(\mu_m + \delta_{ma} + \lambda_m + \gamma_m) + \lambda_3\delta_{ma} + \lambda_5\lambda_m(1-H_m)(1-B_m) + \lambda_{13}\lambda_m$. Thus, $\lambda_2' = -\frac{\partial \mathbf{H}}{\partial S_m} = \lambda_2(\mu_m + \delta_{ma} + \lambda_m + \gamma_m) - \lambda_3\delta_{ma} - \lambda_5\lambda_m(1-H_m)(1-B_m) - \lambda_{13}\lambda_m$, give the second equation of the system (3.5).

The next one is, $\frac{\partial \mathbf{H}}{\partial S_a} = -\lambda_3(\mu_a + \lambda_a + \gamma_a) + \lambda_6\lambda_a(1-H_a)(1-B_a) + \lambda_{14}\gamma_a$. So, $\lambda_3' = -\frac{\partial \mathbf{H}}{\partial S_a} = \lambda_3(\mu_a + \lambda_a + \gamma_a) - \lambda_6\lambda_a(1-H_a)(1-B_a) - \lambda_{14}\gamma_a$, which acts as the third equation of the the system (3.5).

In a similar way, we get:

$$\frac{\partial \mathbf{H}}{\partial E_c} = -\lambda_4(\mu_c+\tau_c+\gamma_c)+\lambda_7\tau_c, \quad \frac{\partial \mathbf{H}}{\partial E_m} = -\lambda_5(\mu_m+\tau_m+\gamma_m)+\lambda_8\tau_m, \quad \frac{\partial \mathbf{H}}{\partial E_a} = -\lambda_6(\mu_a+\tau_a+\gamma_a)+\lambda_9\tau_a.$$

Thus, $\lambda_4' = -\frac{\partial \mathbf{H}}{\partial E_c}$, $\lambda_5' = -\frac{\partial \mathbf{H}}{\partial E_m}$, $\lambda_6' = -\frac{\partial \mathbf{H}}{\partial E_a}$, gives the next three equations of the system (3.5). From the infected compartments:

$$\frac{\partial \mathbf{H}}{\partial I_c} = -\lambda_7(\mu_c+d_c+\alpha_c+\gamma_c)+\lambda_{10}\alpha_c, \frac{\partial \mathbf{H}}{\partial I_m} = -\lambda_8(\mu_m+d_m+\alpha_m+\gamma_m)+\lambda_{10}\alpha_m, \frac{\partial \mathbf{H}}{\partial I_a} = -\lambda_9(\mu_a+d_a+\alpha_a+\gamma_a)+\lambda_{10}\alpha_a.$$

Hence, $\lambda_7' = -\frac{\partial \mathbf{H}}{\partial I_c}$, $\lambda_8' = -\frac{\partial \mathbf{H}}{\partial I_m}$, $\lambda_9' = -\frac{\partial \mathbf{H}}{\partial I_a}$, act as the adjoint equations for infected classes. Following the same process, we get the adjoint equations for treatment and vaccinated classes as follows:

$$\lambda_{10}' = -\frac{\partial \mathbf{H}}{\partial T}, \quad \lambda_{11}' = -\frac{\partial \mathbf{H}}{\partial R}, \quad \lambda_{12}' = -\frac{\partial \mathbf{H}}{\partial V_c}, \quad \lambda_{13}' = -\frac{\partial \mathbf{H}}{\partial V_m}, \quad \lambda_{14}' = -\frac{\partial \mathbf{H}}{\partial V_a}.$$

Therefore, collecting all those expressions yields the system (3.5) of adjoint equations.

$$\begin{cases} \frac{\partial \lambda_1}{\partial t} & = (\mu_c + \delta_{cm} + \lambda_c + \gamma_c)\lambda_1 - \lambda_2 \delta cm(1-H_c)(1-B_c)(1-\sigma_1-\sigma_2) \\ & \quad -\lambda_4 \lambda_c (1-H_c)(1-B_c) - \lambda_{12}\gamma_c, \\ \frac{\partial \lambda_2}{\partial t} & = \lambda_2(\mu_m + \delta_{ma} + \lambda_m + \gamma_m) - \lambda_3 \delta_{ma} - \lambda_5 \lambda_m (1-H_m)(1-B_m) - \lambda_{13}\lambda_m, \\ \frac{\partial \lambda_3}{\partial t} & = \lambda_3(\mu_a + \lambda_a + \gamma_a) - \lambda_6 \lambda_a (1-H_a)(1-B_a) - \lambda_{14}\gamma_a, \\ \frac{\partial \lambda_4}{\partial t} & = \lambda_4(\mu_c + \tau_c + \gamma_c) - \lambda_7 \tau_c, \\ \frac{\partial \lambda_5}{\partial t} & = \lambda_5(\mu_m + \tau_m + \gamma_m) - \lambda_8 \tau_m, \\ \frac{\partial \lambda_6}{\partial t} & = \lambda_6(\mu_a + \tau_a + \gamma_a) - \lambda_9 \tau_a, \\ \frac{\partial \lambda_7}{\partial t} & = \lambda_7(\mu_c + d_c + \alpha_c + \gamma_c) - \lambda_{10}\alpha_c, \\ \frac{\partial \lambda_8}{\partial t} & = \lambda_8(\mu_m + d_m + \alpha_m + \gamma_m) - \lambda_{10}\alpha_m, \\ \frac{\partial \lambda_9}{\partial t} & = \lambda_9(\mu_a + d_a + \alpha_a + \gamma_a) - \lambda_{10}\alpha_a, \\ \frac{\partial \lambda_{10}}{\partial t} & = \lambda_{10}(\mu_h + \gamma_h) - \lambda_{11}\gamma_h, \\ \frac{\partial \lambda_{11}}{\partial t} & = \lambda_{11}(\mu_1 + \phi) - \lambda_{12}\phi_1 - \lambda_{13}\phi_2 - \lambda_{14}\phi_3 - \lambda_1\sigma_1(1-H_C)(1-B_c) \\ & \quad -\lambda_2 \epsilon \delta_{cm} S_c (1-\sigma_1-\sigma_2)\epsilon(1-H_m)(1-B_m) - \lambda_3 \epsilon \sigma_1 (1-H_a)(1-B_a), \\ \frac{\partial \lambda_{12}}{\partial t} & = \lambda_{12}\mu_c, \\ \frac{\partial \lambda_{13}}{\partial t} & = \lambda_{13}\mu_m, \\ \frac{\partial \lambda_{14}}{\partial t} & = \lambda_{14}\mu_a. \end{cases} \tag{3.5}$$

3.4.1 Optimal Control Analysis

The findings from (3.5) is applied to examine the presence of the optimal control framework (3.4). When the following requirements are met, the result of (3.5) can be applied to the optimal control framework (3.4), as it is evident that it is bounded above.

C_1: The set of state variables is present.

C_2: The associated set of admissible control is both closed and convex.

C_3: The right hand side of the control model (3.4) depends linearly on the control variables.

C_4: For $n > 1$, there exist two non-negative constants m_1 and m_2 such that the integrand $\Gamma(\mathbf{x}, B_i, H_i)$ of (B.1) is convex and satisfies the condition below:

$$\Gamma(\mathbf{x}, B_i, H_i) \geq m_2 + m_1 \left(|B_i|^2 + |H_i|^2\right)^{\frac{n}{2}} \text{ with } \Gamma(\mathbf{x}, B_i, H_i) = I_i + C_{H_i} H_i^2 + c_{B_i} B_i^2,\ i = c, m, a.$$

At this stage, the previous study (3.1) is guaranteed, involving state and control variables that are restricted and non-void, satisfying the assumption, C_1. Then, for satisfying the assumption C_2, at first we need to show that the control variables are bounded. To act accordingly, let consider the admissible control set

$$\Gamma = \{(B_i, H_i) \mid 0 \leq B_i \leq 1,\ 0 \leq H_i \leq 1,\ i = c, m, a\}.$$

By the definition of Γ, we can say that each control variable is restricted within the closed interval $[0, 1]$. Therefore, for all admissible controls, we can write:

$$|B_i(t)| \leq 1, \quad |H_i(t)| \leq 1, \quad \forall t \in [0, T],\ i = c, m, a.$$

From the above relations, we get a clear idea that both $B_i(t)$ and $H_i(t)$ are uniformly bounded functions on the time interval $[0, T]$. Hence, there exists a constant $M > 0$ such that

$$\max\{|B_i(t)|, |H_i(t)|\} \leq M, \quad \max\{|B_i(t)|\} \leq M, \quad \max\{|H_i(t)|\} \leq M \quad \forall t \in [0, T].$$

Therefore, the control variables $B_i(t)$ and $H_i(t)$ are bounded in the admissible control set Γ. Consequently, the assumption C_2 is satisfied by the virtue of control set Γ. Given that, the state equations are linear in the control variables B_c, B_m, B_a and H_c, H_m, H_a, the third condition C_3 is satisfied. At the end, it follows that integrand Γ exhibits convexity regarding control steps, B_c, B_m, B_a and H_c, H_m, H_a. For $n > 1$, to show that the integrand remains bounded Γ, suppose $n = 2$, $m_1 = \min(C_{H_i}, C_{B_i})$, and $m_2 = \min(I_c, I_m, I_a)$, afterward, we have

$$\Gamma(\mathbf{x}, B_i, H_i) = I_i + C_{H_i} H_i^2 + C_{B_i} B_i^2 \geq m_2 + m_1 \left(|B_i|^2 + |H_i|^2\right)^{\frac{\pi}{2}},$$

where $i = c, m, a$; $C_{H_i}, C_{B_i}, m_1, m_2 > 0$ and $n > 1$. Hence, we obtained the result.

Theorem 1. *B_i^* and H_i^* constitute the optimal control pair for the model (3.4), in which*

$$(B_i^*, H_i^*) = J_\Gamma min(B_i, H_i)$$

Now, we solve these equations for B_c, B_m, B_a and H_c, H_m, H_a,

$$\begin{cases} \frac{\partial H}{\partial H_c} & = 2C_{H_c} H_c - \lambda_1 \sigma_1 \epsilon R(1 - B_c) - \lambda_4 \lambda_c S_c(1 - B_c) = 0, \\ \frac{\partial H}{\partial H_m} & = 2C_{H_m} H_m - \lambda_2 \delta_{cm} S_c(1 - \sigma_1 - \sigma_2)\epsilon R(1 - B_m) - \lambda_5 \lambda_m S_m(1 - B_m) = 0, \\ \frac{\partial H}{\partial H_a} & = 2C_{H_a} H_a - \lambda_3 \sigma_1 (1 - B_a)\epsilon R - \lambda_6 \lambda_a S_a(1 - B_a) = 0, \\ \frac{\partial H}{\partial B_c} & = 2C_{B_c} B_c - \lambda_1 \sigma_1 \epsilon R(1 - H_c) - \lambda_4 \lambda_c S_c(1 - H_c) = 0, \\ \frac{\partial H}{\partial B_m} & = 2C_{B_m} B_m - \lambda_2 \delta_{cm} S_c(1 - \sigma_1 - \sigma_2)\epsilon R(1 - H_m) - \lambda_5 \lambda_m S_m(1 - H_m) = 0, \\ \frac{\partial H}{\partial B_a} & = 2C_{B_a} B_a - \lambda_3 \sigma_1 (1 - H_a)\epsilon R - \lambda_6 \lambda_a S_a(1 - H_a) = 0. \end{cases}$$

Solving these:

$$\begin{cases} H_c^* & = \frac{\lambda_1 \sigma_1 \epsilon R(1-B_c) + \lambda_4 \lambda_c S_c(1-B_c)}{2C_{H_c}} = A, \\ H_m^* & = \frac{\lambda_2 \delta_{cm} S_c \epsilon R(1-\sigma_1-\sigma_2)(1-B_m) + \lambda_5 \lambda_m S_m(1-B_m)}{2C_{H_m}} = B, \\ H_a^* & = \frac{\lambda_3 \sigma_1 \epsilon R(1-B_a) + \lambda_6 \lambda_a S_a(1-B_a)}{2C_{H_a}} = C, \\ B_c^* & = \frac{\lambda_1 \sigma_1 \epsilon R(1-H_c) + \lambda_4 \lambda_c S_c(1-H_c)}{2C_{B_c}} = D, \\ B_m^* & = \frac{\lambda_2 \delta_{cm} S_c \epsilon R(1-\sigma_1-\sigma_2)(1-H_m) + \lambda_5 \lambda_m S_m(1-H_m)}{2C_{B_m}} = E, \\ B_a^* & = \frac{\lambda_3 \sigma_1 \epsilon R(1-H_a) + \lambda_6 \lambda_a S_a(1-H_a)}{2C_{B_a}} = F. \end{cases}$$

Since, controls are bounded between 0 and 1, then

$$\begin{cases} H_c^*(t) & = \max(0, \min(1, A)), \\ H_m^*(t) & = \max(0, \min(1, B)), \\ H_a^*(t) & = \max(0, \min(1, C)), \\ B_c^*(t) & = \max(0, \min(1, D)), \\ B_m^*(t) & = \max(0, \min(1, E)), \\ B_a^*(t) & = \max(0, \min(1, F)). \end{cases}$$

3.4.2 Optimal Control Characterization

Theorem 1. *Evaluate the controls B_i, H_i, $i = c, m, a$ for the control framework (3.4) involving the optimal results $S_c^*, S_m^*, S_a^*, E_c^*, E_m^*, E_a^*, I_c^*, I_m^*, I_a^*, T^*, R^*, V_c^*, V_m^*$ and V_a^*. Subsequently, the adjoint system is represented by (3.5) and the adjoint variables are λ_i, $i = 1, 2, 3, \cdots, 14$, which satisfy the transversality conditions,*

$$\lambda_i(T_f) = 0 \ \forall \ i = 1, 2, 3, \cdots, 14.$$

Following the minimization of the Hamiltonian **H** *and making sure the adjoint variables vanish after*

time T_f, the controls are identified and deduct the ideal measures for $B_i(t)$ and $H_i(t)$.

$$\begin{cases} H_c^*(t) &= \max(0, \min(1, \frac{\lambda_1\sigma_1\epsilon R(1-B_c)+\lambda_4\lambda_c S_c(1-B_c)}{2C_{H_c}})), \\ H_m^*(t) &= \max(0, \min(1, \frac{\lambda_2\delta_{cm}S_c\epsilon R(1-\sigma_1-\sigma_2)(1-B_m)+\lambda_5\lambda_m S_m(1-B_m)}{2C_{H_m}})), \\ H_a^*(t) &= \max(0, \min(1, \frac{\lambda_3\sigma_1\epsilon R(1-B_a)+\lambda_6\lambda_a S_a(1-B_a)}{2C_{H_a}})), \\ B_c^*(t) &= \max(0, \min(1, \frac{\lambda_1\sigma_1\epsilon R(1-H_c)+\lambda_4\lambda_c S_c(1-H_c)}{2C_{B_c}})), \\ B_m^*(t) &= \max(0, \min(1, \frac{\lambda_2\delta_{cm}S_c\epsilon R(1-\sigma_1-\sigma_2)(1-H_m)+\lambda_5\lambda_m S_m(1-H_m)}{2C_{B_m}})), \\ B_a^*(t) &= \max(0, \min(1, \frac{\lambda_3\sigma_1\epsilon R(1-H_a)+\lambda_6\lambda_a S_a(1-H_a)}{2C_{B_a}})), \end{cases} \tag{3.6}$$

where B_i and H_i are the control variables for balanced diet and hygiene respectively.

Proof. To ensure the availability, constraints and convexity of the optimal control approach of our control model, we consider the findings of the paper. Differentiating the Hamiltonian H with respect to state variables, we get equations (3.5): $\frac{d\lambda_1}{dt} = -\frac{\partial \mathbf{H}}{\partial S_c}, \frac{d\lambda_2}{dt} = -\frac{\partial \mathbf{H}}{\partial S_m}, \frac{d\lambda_3}{dt} = -\frac{\partial \mathbf{H}}{\partial S_a}, \frac{d\lambda_4}{dt} = -\frac{\partial \mathbf{H}}{\partial E_c}, \frac{d\lambda_5}{dt} = -\frac{\partial \mathbf{H}}{\partial E_m}, \frac{d\lambda_6}{dt} = -\frac{\partial \mathbf{H}}{\partial E_a}, \frac{d\lambda_7}{dt} = -\frac{\partial \mathbf{H}}{\partial I_c}, \frac{d\lambda_8}{dt} = -\frac{\partial \mathbf{H}}{\partial I_m}, \frac{d\lambda_9}{dt} = -\frac{\partial \mathbf{H}}{\partial I_a}, \frac{d\lambda_{10}}{dt} = -\frac{\partial \mathbf{H}}{\partial T}, \frac{d\lambda_{11}}{dt} = -\frac{\partial \mathbf{H}}{\partial R}, \frac{d\lambda_{12}}{dt} = -\frac{\partial \mathbf{H}}{\partial V_c}, \frac{d\lambda_{13}}{dt} = -\frac{\partial \mathbf{H}}{\partial V_m}, \frac{d\lambda_{14}}{dt} = -\frac{\partial \mathbf{H}}{\partial V_a}$, where $\lambda_i(T) = 0 \ \forall \ i = 1, 2, 3, \cdots, 14$. The characterization of the optimal control, as given in equation (3.6), follows from the condition $\frac{\partial \mathbf{H}}{\partial x_i} = 0, \ i = 1, 2.$ □

4 Results and Discussion

This section offers a thorough investigation of the results of our pneumonia transmission model, which combines data on prevention, effects of vaccination in three different age groups namely- under 5 years, 5–64 years and above 64 years, and other control measures. By means of this multifarious study, we sought to replicate the progression of pneumonia propagation for different age groups, two control measures, efficacy of vaccine, and other management techniques. Here, we will complete the numerical analysis of our modified pneumonia transmission model, solved by fourth order Runge-Kutta method. We have considered the initial values of different populations from the research work [27] and the considered initial values are displayed in the following Table 5.

Table 5: Initial Values of State Variables.

Susceptible population (> 64), $S_a(0)$	2000
Susceptible population (5–64), $S_m(0)$	300
Susceptible population (< 5), $S_c(0)$	2000
Exposed population (> 64), $E_a(0)$	200
Exposed population (5–64), $E_m(0)$	50
Exposed population (< 5), $E_c(0)$	200
Infectious population (> 64), $I_a(0)$	100
Infectious population (5–64), $I_m(0)$	100
Infectious population (< 5), $I_c(0)$	100
Treated population, $T(0)$	100
Recovered population, $R(0)$	100
Total initial population, $N(0)$	5250

Additionally, maximum parameter values are taken from [27], represented in Table 4. Later, literature-based assumed values for the rates of vaccination $(\gamma_c, \gamma_m, \gamma_a)$ are taken as 0.814, 0.03 and 0.23 respectively and also the proportion of the vaccinated population are considered as $V_c = 0.9$, $V_m = 0.3$, $V_a = 0.7$. In paper [27], where the model was investigated without any effect of vaccination, the basic reproduction number was found to be $R_0 = 1.157$, for which the disease would become epidemic. But after using the vaccination, the basic reproduction number becomes $R_0 = 0.298$, which describes that the rate of spreading disease will become almost negligible.

4.1 Global Sensitivity Analysis

In Table 6, influential parameters are accompanied with Latin Hypercube Sampling – Partial Rank Correlation Coefficient (LHS-PRCC) [30], [32] values that we have used in our comprehensive pneumonia

transmission model (3.1). Thus, the mentioned method enables the identification of critical parameters influencing R_0 and supports the formulation of control strategies that reduce disease burden.

Table 6: PRCC values of the most influential parameters in the proposed pneumonia model (3.1).

Parameter	PRCC Value	Parameter	PRCC Value
β_c	1.0000	μ_m	-0.0631
β_m	0.0048	μ_a	-0.0295
β_a	0.0398	d_c	-0.0253
τ_c	0.0682	d_m	-0.0095
τ_m	0.0696	d_a	-0.0182
τ_a	0.0117	γ_c	-0.0998
α_c	-0.0173	γ_m	-0.0439
α_m	-0.0068	γ_a	-0.0102
α_a	-0.0013	η	0.0672
μ_c	-0.0083		

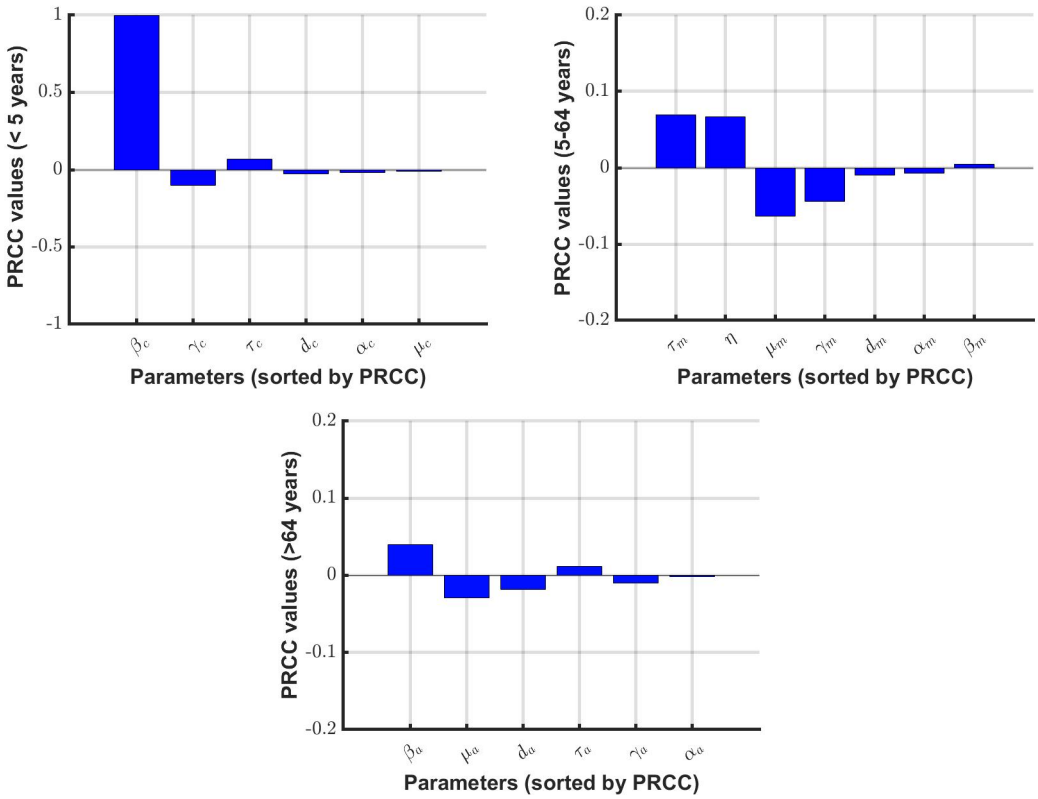


Figure 4: LHS-PRCC values of parameters for the specific age groups.

The LHS- PRCC [32] values have been analyzed for parameters divided into three categories: under 5 years, 5-64 years, and above 64 years and are illustrated in Figure 4. Investigation of Table 6 and graphical representation confirms the highest sensitivity of the contact rate for children i.e β_c, with PRCC of 1.0000, revealing that increases in this parameter are associated with significant increases in R_0. The extremely high value suggests that even a minor increase in β_c substantially elevates the transmission among children. Therefore, reducing exposure and limiting contact within this highly vulnerable age group is crucial. Other parameters showing moderate effects are child vaccination rate

$\gamma_c = -0.0998$, child progression rate τ_c (0.0682), and child specific mortality rate d_c (-0.0253). The negative value suggests that higher disease-induced deaths reduce the number of infectious individuals, thereby limiting transmission.

For the age 5-64 age group, the contact rate β_m (0.0048) displays a very small positive correlation, indicating limited sensitivity in comparison to the younger group. Besides, moderate positive effects are observed for the modification parameter η (0.0672) and the progression rate τ_m (0.0696), which slightly increase transmission by moving individuals from exposed to infectious states. On the contrary, small negative correlations are observed for the treatment rate α_m (-0.0068), natural death rate μ_m (-0.0631), suggesting that improved treatment and natural demographic turnover help decrease the overall infection burden, though the magnitude of influence is weak. Again, the vaccination rate γ_m (-0.0439) also exhibits a small negative impact, indicating that increasing vaccination efforts contributes marginally to reduce transmission.

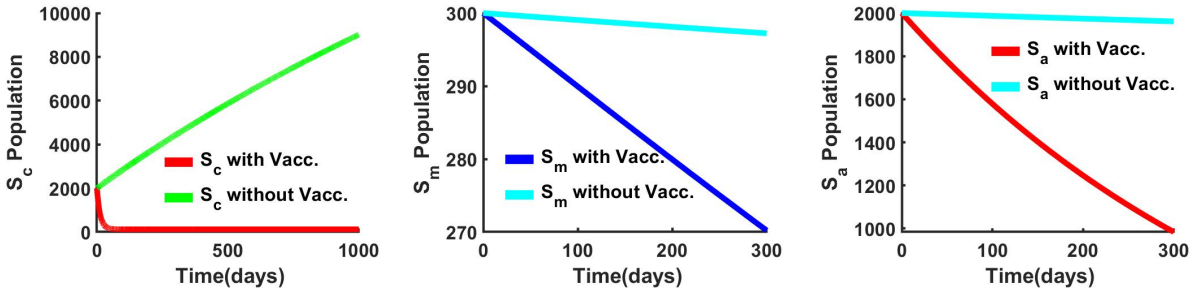
For adults over 64, the contact rate β_a (0.0398) remains the most notable factor, though its influence is weaker than the younger group. Other parameters, progression rate τ_a (0.0117), disease-induced death d_a (-0.0182), vaccination rate γ_a (-0.0102), natural death rate μ_a (-0.0295), and treatment α_a (-0.0013) exhibit very small effects, showing that transmission in this age group is less sensitive to clinical outcomes and more influenced by exposure patterns. Overall, the child contact rate β_c is the dominant driver of transmission sensitivity. For the 5-64 age group, the progression rate τ_m is the most influential, while for adults over 64, the strongest effects arise from β_a. Other parameters show comparatively low sensitivity across all groups. These outcomes highlight the importance of reducing effective contact in younger children, managing progression and infectiousness in adults, and improving vaccination coverage among elderly individuals to effectively control disease transmission.

At this stage, to provide a more meaningful interpretation of the sensitivity analysis, we discuss the public health implications, the role of control variables, and the corresponding intervention strategies derived from the PRCC results. The high sensitivity of the contact rate parameter β_i, particularly β_c, implies that pneumonia transmission is strongly driven by effective contact among individuals, especially children. This indicates that environments where frequent close interactions occur, such as parks, markets, schools, and households, are major contributors to the spread of the disease. Therefore, even a small reduction in the contact rate can lead to a substantial decrease in the basic reproduction number R_0, which confirms the necessity of limiting transmission opportunities in high-contact settings.

The negative PRCC values associated with treatment rates (α_c, α_m, α_a) and vaccination rates (γ_c, γ_m, γ_a) suggest that increasing these control measures leads to a reduction in R_0. This occurs due to a decrease in the number of infectious individuals and a reduction in the infectious period. Hence, treatment and vaccination act as effective mechanisms for controlling disease transmission and reducing the overall disease burden across all age groups. Furthermore, the sensitivity analysis indicates age-specific intervention strategies. Reducing the contact rate β_i through improved hygiene, awareness programs, and reduced overcrowding is important, especially for children. Vaccination is identified as an effective control measure across all age groups, with the strongest impact observed in children. For the other two groups, middle-aged and adult populations, a combined strategy involving vaccination together with preventive measures such as a balanced diet and hygienic practices acts as an effective control approach. These findings highlight that integrating vaccination with behavioral and preventive interventions is essential for reducing pneumonia transmission.

4.2 A Comparative Analysis of the Existing and Modified Model

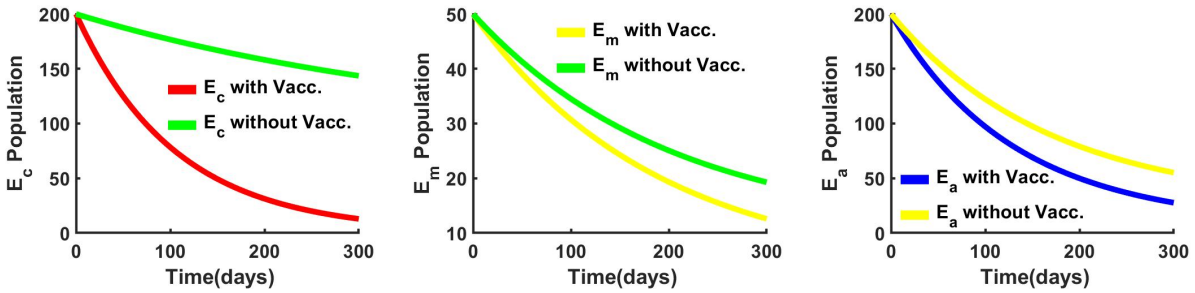
To evaluate the impact of vaccination we compare the models: first one is the existing model (A.1) without vaccination and the second one is the modified model (3.1) with vaccination. The models (A.1) and (3.1) were solved numerically using MATLAB via Runge-Kutta fourth order method.



(a) (b) (c)

Figure 5: S_c, S_m, and S_a populations of previous (A.1) and developed (3.1) models.

In Figure 5, the comparative analysis for the susceptible population under 5 (S_c) between the existing and modified models is noticeable. After applying vaccination, it decreases S_c population, causing immunity. It effectively diminishes the individuals who are vulnerable to infection. So, the difference in S_c can be seen transparently. Also, vaccination lowers the susceptible population for middle age (S_m), inducing immunity. For S_m, vaccination affects the spread and monotonically decreases the susceptible individuals. Moreover, the difference between the middle-aged susceptible individuals without and with vaccination is significant. Susceptible population for adults (S_a) also maintains a characteristic harmony with S_c and S_m. After incorporating vaccination, S_a declined dramatically, reducing the pool of individuals susceptible to infection, as also demonstrated in Figure 5. Observing the above description and clear differences after the introduction of vaccination, as supported by Figure 5, we can interpret that the susceptible populations in three age groups: S_c, S_m, and S_a declined from approximately 2000, 300, and 2000 to about 285, 270, and 985 after 300 days. Before the implementation of vaccination, the susceptible populations change from approximately 2000 to 2263 for S_c, from 300 to 290 for S_m, and from 2000 to 1960 for S_a at time $t = 300$ days. Therefore, the reductions in S_c, S_m, and S_a with vaccination are approximately 90%, 9%, and 50% greater, respectively, than in the scenario without vaccination. These results indicate that vaccination is most effective for children under five years (S_c), followed by adults, and least effective for the middle-aged group. Overall, this highlights that immunization plays a vital role in reducing and potentially eradicating the disease within a community.

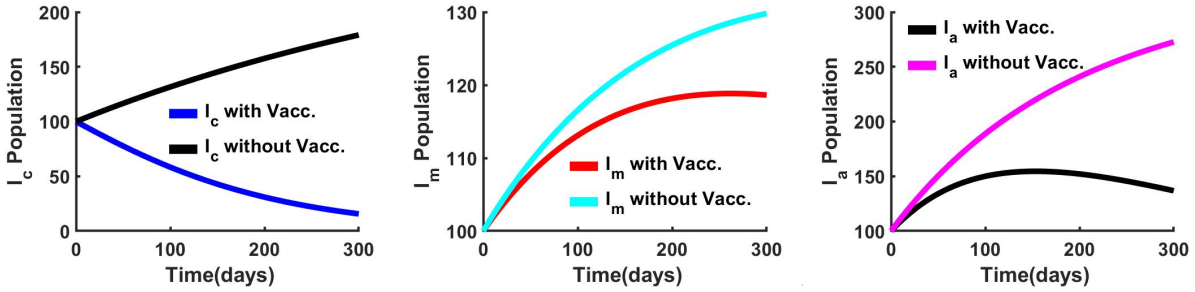


(a) (b) (c)

Figure 6: E_c, E_m, and E_a populations of previous (A.1) and developed (3.1) models.

In Figure 6, we compared the exposed population of the previous study (A.1) and the developed study (3.1). After using vaccination, there exists some differences in the exposed population for children (E_c), middle-aged (E_m), and adults (E_a). From Figure 6, it is transparent that the E_c, E_m, E_a populations of the vaccinated model have been lessened compared to the existing model, especially for E_c. Due to vaccination, the exposed population will reduce drastically, which can also be supported by Figure 6. Additionally, the exposed populations E_c, E_m, and E_a declined approximately from 200 to 12, 50 to 13, and 200 to 27, respectively at 300 days, due to the incorporation of vaccination. However, before the implementation of vaccination, the exposed populations reduce naturally to approximately 143, 20, and 55 at time $t = 300$ days. Therefore, compared to the scenario without vaccination, the

reductions in E_c, E_m, and E_a under vaccination are approximately 90%, 8%, and 50% greater, respectively, indicating that vaccination is most effective among exposed children, followed by the adults, and least effective among the middle ages group. These results for the exposed population are consistent with the observed impact of vaccination on the susceptible population. Hence, we conclude that, in the absence of vaccination, it is difficult to control the disease, whereas vaccination serves as an effective strategy to limit the spread among susceptible and exposed individuals by significantly reducing their numbers. Therefore, both Figures 5 and 6 demonstrate the effectiveness of vaccination in controlling the infectious disease.



(a) (b) (c)

Figure 7: I_c, I_m, I_a populations of previous (A.1) and developed (3.1) models.

Figure 7 presents a comparison of the infected populations across the three age groups with and without vaccination. We observe that, in the absence of vaccination, the populations of I_c, I_m, and I_a increase to approximately 180, 130, and 270, respectively, over a period of 300 days, while the initial population in each case was 100. This indicates a significant rise in the infected population without vaccination. In contrast, vaccination reduces the number of infected individuals, as illustrated in Figure 7. So, we observe the reduction in infected population for children, middle aged and adults (I_c, I_m, I_a) after introducing vaccination, is considerable. The infection rates for I_c, I_m, I_a have reduced intensely. Vaccination affects the infection rate a lot which we can be justified from the comparison Figure 7 of the baseline model and proposed model. After incorporating vaccination, the populations of I_c, I_m, and I_a are approximately reduces to 15, 118, and 136, respectively. Therefore, the reductions in I_c, I_m, and I_a with vaccination are approximately 91%, 9%, and 49% greater, respectively, than in the scenario without vaccination. In addition, vaccination not only reduces the peak size of the infected populations but also delays and smooths the trajectories of the infection curves. Here, vaccination is most influential for I_c and I_a compared to I_m. This indicates that vaccination reduces the transmission intensity, resulting in a more stable and gradual decline in infected individuals across all age groups.

The comparison between models (3.1) and (A.1) indicates that incorporating vaccination leads to a significant reduction in the susceptible, exposed, and infected populations across all age groups. The revised model exhibits a faster decline and lower levels in these compartments compared to the existing model, showing its greater effectiveness in limiting disease transmission. These outcomes underscores the importance of including vaccination for a more realistic representation of epidemic dynamics. Moreover, vaccination shows greater effectiveness for children, followed by adults and then middle-aged individuals, across the susceptible, exposed, and infected compartments, indicating that vaccination is comparatively more important for vulnerable or high-risk populations.

4.3 Impact of Parameter Variation

We explore the impacts of parameters on the extensive pneumonia proposed model (3.1). τ_c, τ_m and τ_a are the progression rates for I_c, I_m and I_a respectively. Again, μ_m is the natural death rate for people between 5 and 64 age. Additionally, β_c and β_m are contact rates for I_c and I_m respectively. We will examine each parameter under three scenarios: the original model values, together with one reduced and one increased value, to reflect possible variations in biological behaviors.

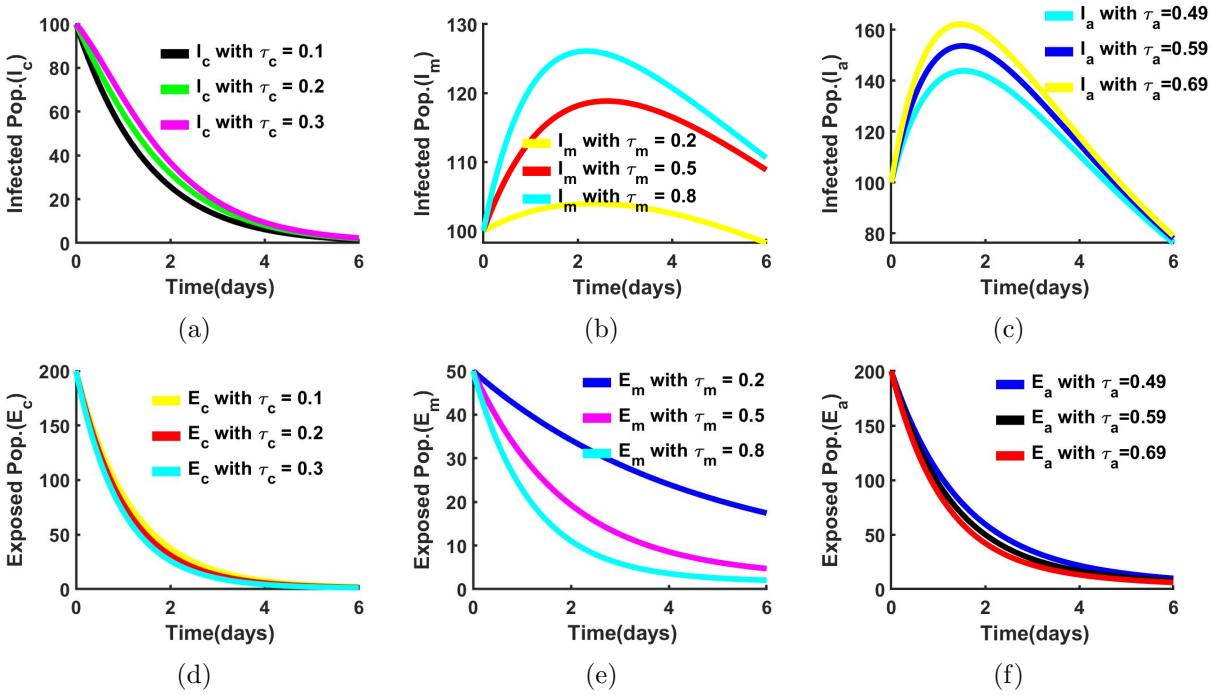


Figure 8: The effects of τ_c, τ_m and τ_a on infected and exposed populations of model (3.1).

Figure 8 demonstrates how variations in the progression rates determine the speed at which individuals move from the exposed class to the infectious class. For I_c, I_m, and I_a, the values of τ_c, τ_m, and τ_a are taken as $(0.1, 0.2, 0.3)$, $(0.2, 0.5, 0.8)$, and $(0.49, 0.59, 0.69)$, respectively. Additionally, for E_c, E_m, and E_a, the same sets of values are considered as those used for I_c, I_m, and I_a. Higher values of the progression parameters lead to a quicker reduction in the exposed individuals and an earlier increase in infections. More specifically, sub-figures (8a-8c) illustrates the impact of varying τ_c, τ_m, and τ_a on the infected population across children, middle aged and adults groups, respectively. An increase in these parameters leads to a quicker and higher infection peak. On the other hand, sub-figures (8d-8f) show the corresponding behavior in the exposed population, where higher progression rates lead to a faster decline, indicating a shorter incubation period. Among the three age groups, changes in progression rate for people between 5 and 64 age i.e τ_m produce the most noticeable shifts in both exposed and infected trajectories which we can see from Figures 8b and 8e.

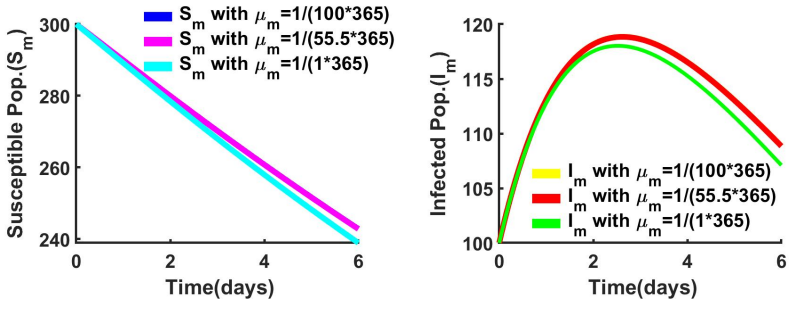
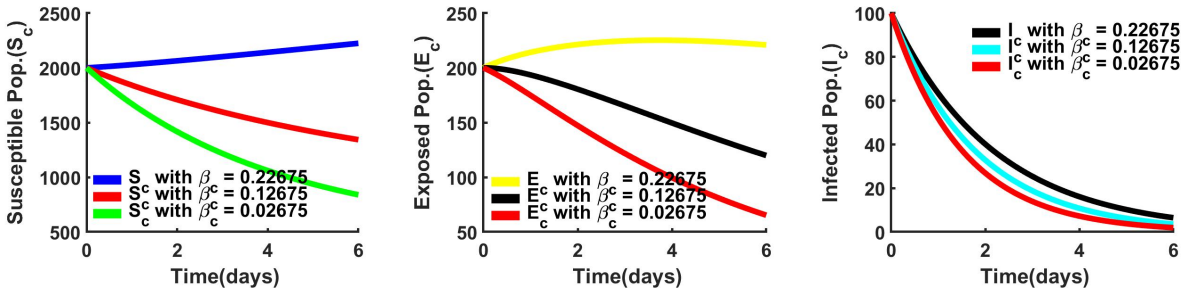


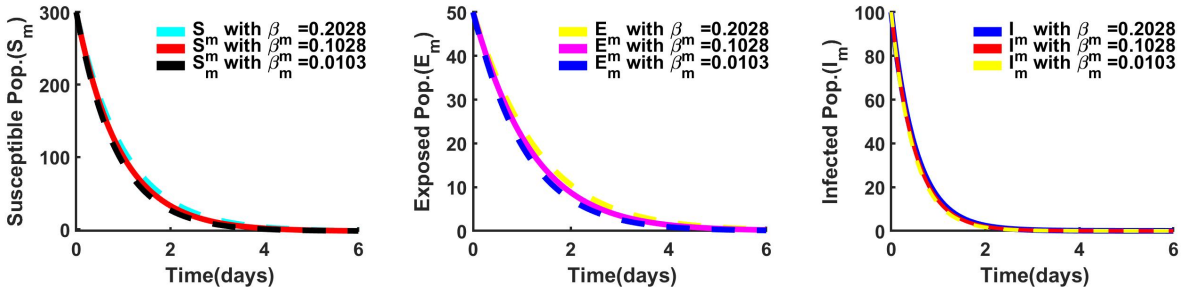
Figure 9: The effects of μ_m on susceptible and infectious populations of model (3.1).

Again, Figures 9a-9b explores how different natural death rates for individuals aged 5-64 affect disease dynamics. As the value of μ_m increases, the susceptible population decline rapidly, while the infectious population shows modest reductions in peak levels. These results suggest that natural death mainly decreases the number of susceptible individuals and does not greatly affect how the disease spreads.



(a) (b) (c)

Figure 10: The effects of β_c for susceptible, exposed and infected populations of model (3.1).



(a) (b) (c)

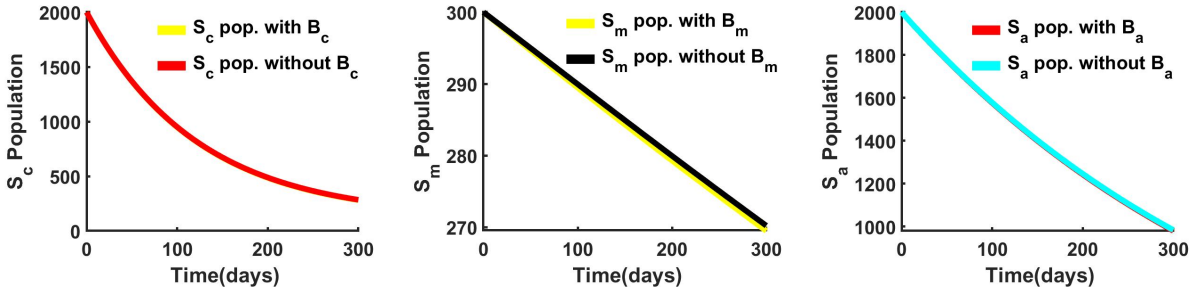
Figure 11: The effects of β_m for susceptible, exposed and infected populations of model (3.1).

The effects of varying the contact rate among children is highlighted in Figure 10. For S_c, E_c, and I_c, the considered values of the contact rates are $(0.22675, 0.12675, 0.02675)$ for each population. Higher contact rates cause a corresponding rise in all susceptible, exposed and infected individuals. This exhibits the largest variation across scenarios, indicating that transmission among children is highly sensitive to changes in β_c. For I_c and E_c, this difference is significant; higher values of β_c lead to a greater increase in the S_c and E_c populations, followed by I_c. On the other hand, Figure 11 illustrates the contact rate among individuals aged 5-64. Here, the values of β_m are taken as $(0.2028, 0.1028, 0.0103)$ for S_m, E_m, and I_m, respectively. Under this variation, all middle-aged populations exhibit similar behavior. Increasing β_m accelerates the increase in all individuals like as β_c but the effect is milder. The effects vary by age group. The progression rate (τ_i) has a more pronounced effect on the middle-aged and adult populations, particularly for I_m, I_a, E_m, and E_a, whereas the contact rate (β_i) plays a more significant role in influencing the child and early-stage exposed populations, such as S_c and E_c, with comparatively milder effects on the remaining parameters. Therefore, the analysis of parameter variations shows that both progression and contact rates play a significant role in shaping the dynamics of the susceptible, exposed, and infected populations across different age groups. These findings highlight the importance of appropriate parameter selection for accurately capturing and interpreting disease transmission dynamics.

4.4 Optimal Control Strategies

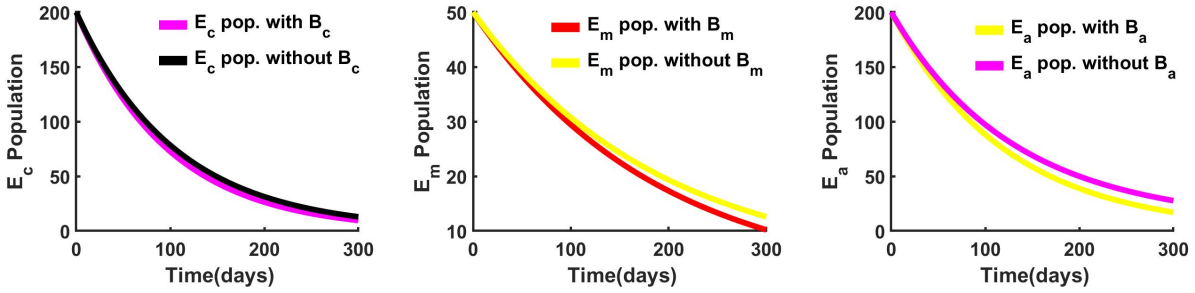
This section will discuss the numerical results of the modified model with control and without control. Here, we used two factors: balance diet(B_c, B_m, B_a) and hygiene (H_a, H_m, H_a) for three different age groups. We used fourth order Runge-Kutta method to find the solution of optimal control model using MATLAB code.

Case-1: Balanced diet only (B_c, B_m, B_a)



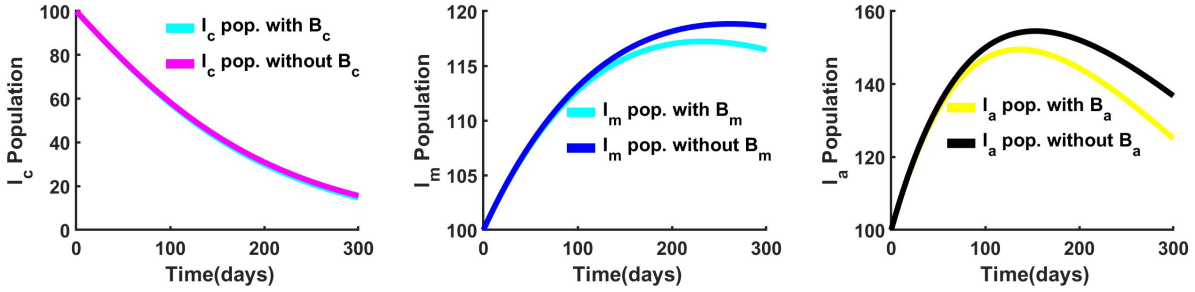
(a) (b) (c)

Figure 12: Numerical configuration for susceptible populations of model (3.4) using balanced diet only.



(a) (b) (c)

Figure 13: Numerical configuration for exposed populations of model (3.4) using balanced diet only.



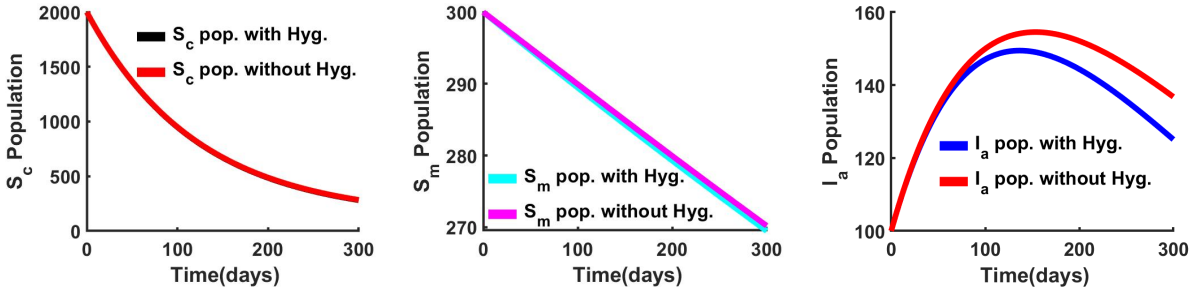
(a) (b) (c)

Figure 14: Numerical configuration for infectious population of model (3.4) using balanced diet only.

In case-1, we have considered nonzero values of $B_c, B_m,$ and B_a whereas $H_c = H_m = H_a = 0$, which means that only the balanced diet is considered as a control for all age groups. This case is described in Figures 12, 13, and 14, where the susceptible (S_c, S_m, S_a), exposed (E_c, E_m, E_a), and infected (I_c, I_m, I_a) populations are presented, respectively, over the time interval $t \in [0, 300]$. In Figure 12, for the susceptible population across all age groups, there is no significant change after applying the balanced diet control. From this figure, it is clear that after adding vaccination, the S_c population reduces from 2000 to around 285, and after implementing the control measure (balanced diet), it reduces by a very small

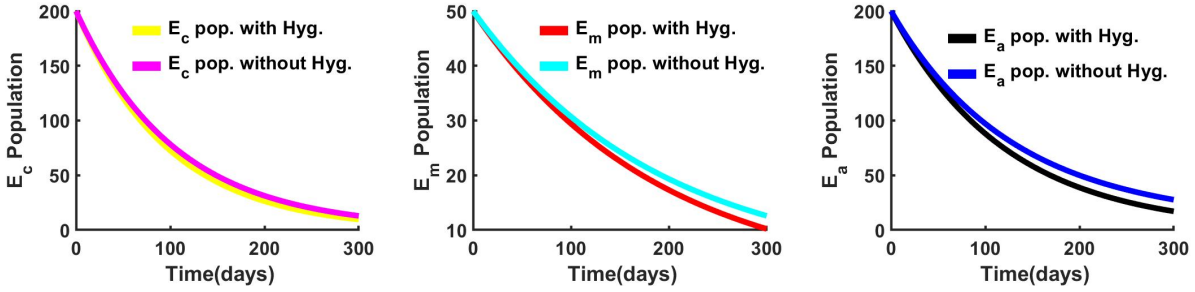
amount to approximately 280. For S_m, the difference is also not noticeable, similar to S_c. Then, for S_a, the reduction due to vaccination is from 2000 to around 985, and for the balanced diet it reduces to approximately 980, which is not remarkable. Next, for the exposed population, a slight reduction is observed in the child group, while the middle-aged and adult groups show a more noticeable decrease in the exposed population due to the application of the balanced diet control which we can see from the Figure 13. Observing Figure 13, we can say that the reduction due to the implementation of balanced diet in the exposed population for E_a is the highest, approximately 38%, compared to E_c and E_m, which are approximately 19% and 26%, respectively. Figure 14 presents the comparison of the infectious population with and without the balanced diet intervention. This figure displays a different scenario from Figure 12 and is quite similar to Figure 13. Observing these two figures, we can say that although the susceptible populations do not show any noticeable difference between the balanced diet and non-balanced diet cases, the exposed and infected populations of all age groups (E_c, E_m, E_a and I_c, I_m, I_a) show higher reductions compared to the susceptible population. For the infected population under the age of 5, the decline is minimal; however, the middle-aged and adult populations show noticeable reductions. In addition, the reductions for I_c, I_m, I_a are approximately 1%, 5%, and 7%, respectively. This is likely because children under 5 years can not maintain a proper balanced diet, resulting in limited effects of the control. Therefore, there is not much difference in the susceptible, exposed, and infected populations for this group. In contrast, a greater reduction is observed in both the exposed and infectious populations for the middle-aged and adult groups.

Case-2: Hygiene only (H_c, H_m, H_a)



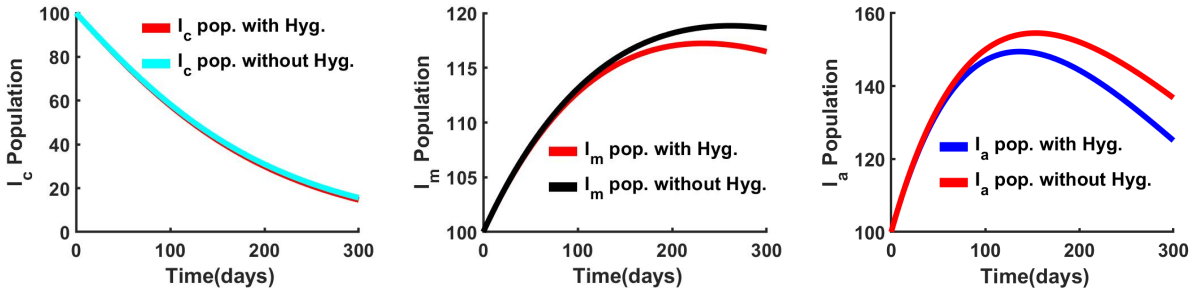
(a) (b) (c)

Figure 15: Numerical configuration of model (3.4) with hygiene and without hygiene for susceptible populations.



(a) (b) (c)

Figure 16: Numerical configuration of model (3.4) with hygiene and without hygiene for exposed populations.



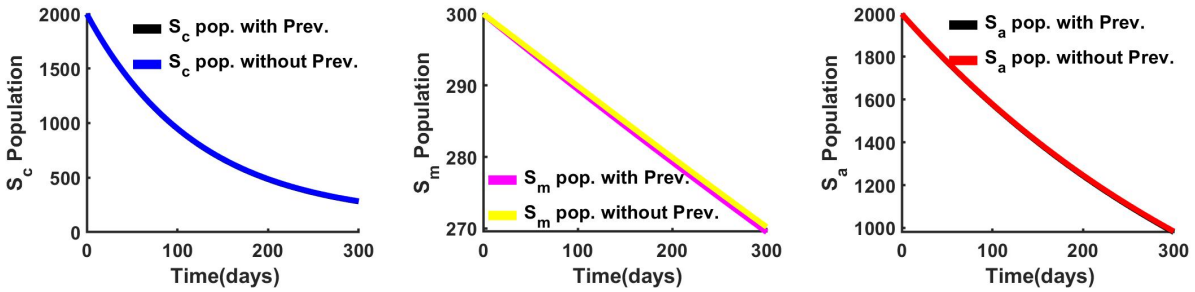
(a) (b) (c)

Figure 17: Numerical configuration of model (3.4) with hygiene and without hygiene for infectious populations.

In case-2, we set $B_c = B_m = B_a = 0$, while H_c, H_m and H_a have nonzero values. In Figures 15-16, we present a comparison between the scenarios with and without the hygiene control for the susceptible and exposed populations. Both child and middle aged groups do not show noticeable changes in the susceptible population after applying this control, while a slight reduction is observed in the adult group. Numerical results show that the initial susceptible populations for S_c, S_m, and S_a are 2000, 300, and 2000 individuals, respectively. Over time, these populations decrease significantly to approximately 285, 270, and 985, respectively, due to the influence of vaccination. However, no substantial reduction is observed under the implementation of hygiene control alone, as the populations remain approximately 280, 265, and 975, respectively, in that case. For the exposed population, we obtain improved results across all age groups. The deductions for E_c, E_m and E_a individuals are from 200, 50, 200 to approximately 12, 15, and 27 due to the effects of vaccination and after control measure it reduces to 9, 10, 15, respectively. Therefore, Figure 16 indicates a significant reduction for E_m and E_a. Moreover, from Figure 17, it is shown that the most substantial reduction occurs in the adult group of infected population, I_a, then for I_m and I_c respectively. Numerically, the reduction percentages are 1%, 6% and 8% for I_c, I_a, I_m respectively.

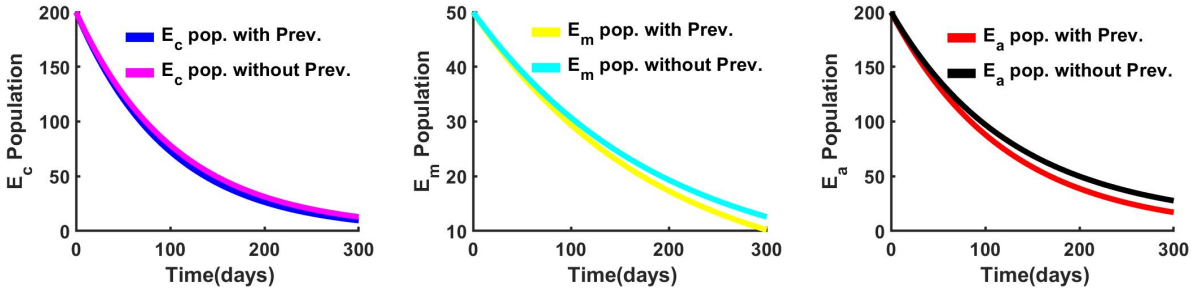
From the analysis of the above two cases, we can summarize that both control strategies are effective for the middle-aged and adult groups, while the child group is not significantly influenced by either intervention. For children under 5 years, vaccination is the most effective control strategy. Based on this comparative assessment, we may conclude that, for the child group, both a balanced diet and maintaining hygiene are important, as a balanced diet enhances immune development and reduces malnutrition, while hygiene practices directly reduce infection. For the middle-aged group, hygienic food is more important and impactful, as it helps prevent pathogen exposure through contaminated food, which is especially relevant for this group with relatively stable immunity. Finally, for the adult group, hygiene practices are more effective because they directly reduce infection transmission, while a balanced diet improves immunity and indirectly slows down infection transmission.

Case-3: Both balance diet (B_c, B_m, B_a) and hygiene (H_c, H_m, H_a)



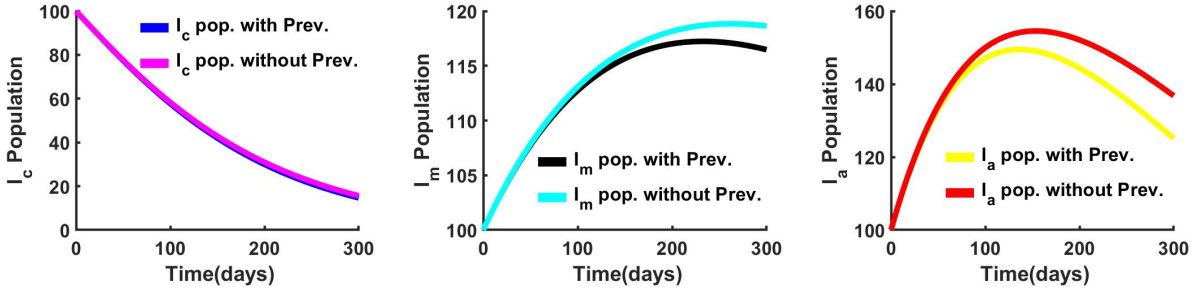
(a) (b) (c)

Figure 18: Numerical configuration for susceptible populations of model (3.4) with both balanced diet and hygiene.



(a) (b) (c)

Figure 19: Numerical configuration for exposed populations of model (3.4) with both balanced diet and hygiene.



(a) (b) (c)

Figure 20: Numerical configuration for infectious population of model (3.4) with both balanced diet and hygiene.

In case-3, we consider nonzero values of B_c, B_m, B_a and H_c, H_m, H_a. Here, a slight reduction in the susceptible population is observed for the middle-aged and adults groups, while the values remain almost unchanged for the children group, as described in Figure 18. For the exposed population, both controls are effective for the middle-aged and adult groups, which is also claimed by Figure 19. The most significant benefit is observed in the infectious population for the middle-aged and adult groups, as shown in Figure 20. The reduction percentages for the infected populations I_c, I_m, and I_a are approximately 3%, 7%, and 9%, respectively, which are comparatively higher than those obtained from any

single control measure. Therefore, we can conclude that applying both preventive measures (balanced diet and hygienic) is the most effective strategy to control pneumonia in the middle-aged and adult populations, though it has limited impact on the child group. Vaccination reduces infection across all age groups, with the greatest effect seen in children, whereas the preventive controls are less effective for this group since they are quite unable to maintain balanced diet and hygiene. Hence, both vaccination and control measures are crucial for protecting the community. Specifically, vaccination plays a more vital role for children, while for the middle-aged and adult groups, a combination of vaccination and preventive controls is most effective.

4.4.1 Comparative Cost-Effectiveness Analysis of Control Strategies

To investigate the comparative performance of the considered intervention strategies, namely balanced diet and hygiene, we evaluate two main performance indices: the total number of infected individuals over the simulation period and the total implementation cost of the control strategies [15]. Here, the cumulative infection burden is calculated as follows:

$$\mathcal{I} = \int_0^T \left(I_c(t) + I_m(t) + I_a(t)\right)\, dt,$$

which measures the overall disease prevalence over time.
Next, the total cost of intervention is defined as:

$$\mathcal{C} = \int_0^T \sum_{i=c,m,a} \left(C_{H_i} H_i^2(t) + C_{B_i} B_i^2(t)\right)\, dt, \tag{4.1}$$

which calculates the cumulative cost of implementing two intervention strategies: balance diet and hygiene.
Moreover, the cost-effectiveness ratio (CER) is the ratio of total cost of intervention for reducing the cumulative infection burden over the time interval $[0, 300]$. A lower CER represents a more cost-effective control strategy.

Table 7: Comparison of control strategies based on cumulative infection burden, total cost, effectiveness, and cost-effectiveness over the time interval $t \in [0, 300]$.

Strategy	Cumulative Infections ($\mathcal{I}$)	Cost ($\mathcal{C}$)	Reduction (%)	CER ($\times 10^3$)	Rank
No control	4448.12	0.00	0.000	–	4
Balanced diet only	3859.41	7829404.19	13.235	591.40	3
Hygiene only	3768.91	7828044.71	15.270	512.69	2
Combined control	3598.71	7821296.81	19.096	409.61	1

Table 7 compares the effectiveness of the proposed intervention strategies in reducing the cumulative infection burden over the time interval $t \in [0, 300]$. It is evident that all control strategies are capable of reducing the infection level. Among the two individual strategies, hygiene performs better than balanced diet alone in terms of both infection reduction and cost-effectiveness, indicating that hygiene-related measures have a stronger impact on reducing disease transmission. However, the combined implementation of both control strategies yields the lowest infection level, confirming its superior epidemiological performance. These findings are also supported by the graphical representations in Figures 14, 17, and 20.

The combined strategy shows the highest reduction in infection burden, leading to a more efficient balance between cost and epidemiological benefit, although all control strategies require substantial implementation costs. Additionally, this observation is supported by the cost-effectiveness analysis measured through the CER. The combined strategy exhibits the lowest CER, indicating that it achieves the greatest reduction in infection per unit cost and is therefore the most cost-efficient strategy among the three considered cases. In contrast, the balanced diet-only strategy shows comparatively lower efficiency due to its highest CER value.

Although these prevention strategies are beneficial, implementing them effectively in low-resource or underserved populations can be challenging due to economic restrictions and limitations in public health infrastructure. In such settings, essential preventive measures like balanced nutrition and hygiene may

be difficult to sustain consistently, which can reduce their practical impact on disease control. In our study, we observed that combining preventive controls (i.e., balanced diet and hygiene) with vaccination significantly enhances overall disease mitigation. Vaccination reduces infection rates across all age groups, especially in children who are more vulnerable and often prioritized in immunization programs. Preventive controls alone may have limited impact in younger children due to practical challenges in maintaining a balanced diet and hygiene among this group, but controls are more effective for other age groups. Therefore, both preventive interventions and vaccination are essential for community protection as well as for low-income areas. However, for such regions, it is quite difficult to ensure the cost for balanced nutrition and maintaining hygiene. Due to this economic challenges, it is very important to make a smooth relationship between implementation difficulties and cost effectiveness for such unprivileged areas. Because of these limitations, our study gives suitable recommendations for the authority to perform an important cost-benefit analysis in unprivileged regions that investigates the highest effective strategy for balancing effectiveness and affordability. Since for underserved populations in low-income regions, it is difficult to implement the controls properly, governments should support their populations by increasing awareness, providing sufficient training, and increasing vaccination coverage with higher efficacy, and governments should take necessary steps in such regions to control the key parameters: progression rates, contact rates, etc.

5 Conclusion

This study successfully demonstrate the transmission dynamics of modified pneumonia model with vaccination, whereas all population compartments are classified into three age groups: children (under 5 years), middle aged (5-64 years) and adults (above 64 years). Firstly, we have verified that the proposed model is forward invariant and well-posed, both mathematically and epidemiologically. Then, using parameters values, we have evaluated the equilibrium points of the modified pneumonia model, then calculated basic reproduction number as $R_0 = 0.298 < 1$, which confirms that the pneumonia for all three age groups will die out from a community after incorporating vaccination. Additionally, the stability analysis of our model was also completed and another important analysis–global sensitivity analysis by calculating LHS-PRCC values, which identify which parameters are working as key parameters for this working mathematical frame. For children, the most effective parameter is β_c–contact rate for children under 5 years, which have a strong positive correlation with R_0. Next, for 5-64 years, the key parameters which have significant impact on this age groups are η = modification parameter, β_m = contact rate, τ_m = progression rate and others have light impact. Moreover, for adults, the most influential parameter is the contact rate, β_a and others have moderate effectiveness over this population group. Following that, the study has obtained an optimal control framework including two interventions: balanced diet and hygiene and applied Pontryagin's Maximum Principle [31] for finding optimized control. We performed numerical simulation in MATLAB using RK4 method, made a comparison between the previous framework without vaccination and the developed framework including vaccination. We have analyzed the correlative relationship between susceptible, exposed and infected populations for three age groups separately, without vaccination versus with vaccination and do the same comparison for E_c, E_m, E_a and I_c, I_m, I_a. Consequently, we observe a substantial reduction in the susceptible, exposed and infected populations. Additionally, we have included variation of parameters where a comparative study has displayed graphically to find the effects of key parameters on different age groups, which is also related and supported by the global sensitivity analysis. Next, three comparisons have been demonstrated graphically for Case-1: $S_c, S_m, S_a, E_c, E_m, E_a, I_c, I_m, I_a$ populations with and without the control balanced diet, Case-2: with and without the control hygiene, Case-3: with and without both controls. These comparisons conclude that for children under 5 years, vaccination is the most important strategy and for middle aged 5-64 years and adults above 64 years, vaccination and both controls are combinedly effective for the eradication of pneumonia disease among both hosts and vector populations. Moreover, a comparative cost-effectiveness analysis of intervention measures ensures that combined control strategies are more cost-effective and epidemiologically efficient in decreasing disease transmission dynamics. The study highlights the importance of robust modeling frameworks in shaping evidence based policies and effective public health strategies to combat pneumonia.

Declarations

Funding: The author, Sadia Akter Lima, acknowledges the financial support of the Noakhali Science and Technology University Research Cell (NSTURC), Noakhali-3814, Bangladesh.

Competing Interests: The authors declare no conflict of interest.

Data Availability: The datasets generated and/or analysed during the current study are available in the Sadia Akter Lima [**sadianstu**] repository, https://github.com/sadianstu/Pneumonia/tree/main.

Ethical Approval: No consent is required to publish this manuscript. There was no Human participants in this study.

Author Contributions: MSR: Data curation; Formal analysis; Methodology; Software; Writing – original draft.
SAL: Conceptualization; Data curation; Formal analysis; Funding acquisition; Supervision; Validation; Writing – original draft, review & editing.
ZHR: Formal analysis; Investigation; Validation; Software; Writing – original draft.
KM: Formal analysis; Methodology; Software; Writing – original draft, review & editing.
MK: Conceptualization; Funding acquisition; Supervision; Resources; Validation; Writing – review & editing.

Appendix

A Baseline Model

The previous model (A.1) is given below,

$$\begin{cases} S_c' &= \Pi_c + \sigma_1 \xi R - (\mu_c + \delta_{cm} + \lambda_c) S_c, \\ S_m' &= \delta_{cm} S_c (1 - \sigma_1 - \sigma_2) \xi R - (\mu_m + \delta_{ma} + \lambda_m) S_m, \\ S_a' &= \delta_{ma} S_m + \sigma_2 \xi R - (\mu_a + \lambda_a) S_a, \\ E_c' &= \lambda_c S_c - (\mu_c + \tau_c) E_c, \\ E_m' &= \lambda_m S_m - (\mu_m + \tau_m) E_m, \\ E_a' &= \lambda_a S_a - (\mu_a + \tau_a) E_a, \\ I_c' &= \tau_c E_c - (\mu_c + d_c + \alpha_c) I_c, \\ I_m' &= \tau_m E_m - (\mu_m + d_m + \alpha_m) I_m, \\ I_a' &= \tau_a E_a - (\mu_a + d_a + \alpha_a) I_a, \\ T' &= \alpha_c I_c + \alpha_m I_m + \alpha_a I_a - (\mu_h + \gamma_h) T, \\ R' &= \gamma_h T - (\mu_h + \phi) R, \end{cases} \tag{A.1}$$

with positive initial conditions,

$$\begin{cases} S_c(0) \geq 0, S_m(0) \geq 0, S_a(0) \geq 0, E_c(0) \geq 0, E_m(0) \geq 0, E_a(0) \geq 0, \\ I_c(0) \geq 0, I_m(0) \geq 0, I_a(0) \geq 0, T(0) \geq 0, R(0) \geq 0. \end{cases} \tag{A.2}$$

In the existing model (A.1), the author suggested three different age groups for the population: under 5 years, 5–64 years and above 64 years. In the model, the total populations are categorized into five epidemiological states, that is, susceptible (S_c, S_m, S_a), exposed (E_c, E_m, E_a), infectious (I_c, I_m, I_a),

treated (T), recovered (R). Hence, the total population for the disease is $N_p = S_c + S_m + S_a + E_c + E_m + E_a + I_c + I_m + I_a + T + R$. The model is mainly based on the population of high risk of pneumonia infection.

B Mathematical Analysis of the Modified Model

We define the admissible domain,

$$\Omega_h = \left\{ (S_c(t), S_m(t), S_a(t), E_c(t), E_m(t), E_a(t), I_c(t), I_m(t), I_a(t), T(t), R(t), V_c(t), V_m(t), V_a(t)) \in \mathbb{R}^{14}+ : N_h(t) \leq \frac{\pi_c}{\mu_c} \right\},$$

and $\Omega = \Omega_h \subseteq \mathbb{R}^{14}_+$. Considering this area, the study produces the following findings.

Lemma B.1. *The fundamental theory of dynamical systems, as outlined in (3.1), can be used to demonstrate the invariant region, well-posedness, non-negativity, and boundedness of solutions of the suggested model.*

Proof. Over the modeling period, the solutions with non-negative initial conditions stay within the neighborhood of the closed positive hyperspace, $\overline{\Omega} = \Omega_h \subseteq \mathbb{R}^{14}_+$, that is, $(S_i, E_i, I_i, T, R, V_i) \in \mathbb{R}^{14}_+$ since,

$$\begin{aligned}
&\frac{dS_c}{dt} = \Pi_c + \sigma_1 \epsilon R \geq 0, \frac{dS_m}{dt} = \delta_{cm} S_c (1 - \sigma_1 - \sigma_2)\epsilon R \geq 0, \frac{dS_a}{dt} = \delta_{ma} S_m + \sigma_1 \epsilon R \geq 0,\\
&\frac{dE_c}{dt} = \lambda_c S_c \geq 0, \frac{dE_m}{dt} = \lambda_m S_m \geq 0, \frac{dE_a}{dt} = \lambda_a S_a \geq 0,\\
&\frac{dI_c}{dt} = \tau_c E_c \geq 0, \frac{dI_m}{dt} = \tau_m E_m \geq 0, \frac{dI_a}{dt} = \tau_a E_a \geq 0,\\
&\frac{dT}{dt} = \alpha_c I_c + \alpha_m I_m + \alpha_a I_a \geq 0, \frac{dR}{dt} = \gamma_h T \geq 0,\\
&\frac{dV_c}{dt} = \gamma_c S_c \geq 0, \frac{dV_m}{dt} = \gamma_m S_m \geq 0, \frac{dV_a}{dt} = \gamma_a S_a \geq 0,
\end{aligned}$$

Adding all the equations of the system, we obtain the following dynamic of the total population

$$\frac{dN_h}{dt} = \pi_- \mu_i N_i - \mu_h (T + R) - d_i I_i + \phi_1 R + \phi_2 R + \phi_3 R, \text{ where } i = c, m, a.$$

Being aware that μ_c is smaller than μ_h, μ_m, and μ_a. The following differential inequality is what we get, $\frac{dN}{dt} \leq \pi_c - \mu_c N_h$, whose solutions is $N(t) \leq \frac{\pi_c}{\mu_h} + (N(0) - \frac{\pi_c}{\mu_c})(e^{-\mu_c t})$. Consequently, the biologically viable zone for Model (3.1) is defined as Ω_h fulfills the theory of differential equations.

$$\Omega_h = \{(S_i, E_i, I_i, T, R, V_i) \in \mathbb{R}^{14}_+ : N_h \leq \tfrac{\pi_c}{\mu_h}\}.$$

In the specified feasible region, Ω_h, the system is positively invariant and attractive. It should be noted that the region Ω_h is positively invariant for model (3.1) based on the inequalities in (3.2). Therefore, the solution trajectories will stay in Ω_h for all time t, given any initial conditions in Ω_h. We can demonstrate that there exists a simple solution of model (3.1) in Ω_h for $t \in [0, \infty)$ for any initial conditions in Ω_h using a common method. Thus, model (3.1) is well-posed both mathematically and epidemiologically. □

B.1 Disease Free Equilibrium points

In this part, we will find the equilibrium points [27, 30, 33] of the model (3.1). To get the disease free equilibrium points (E_0), DFE, we set the right hand side of the model (3.1) equals to zero. In this case,

for equilibrium points:

$$\begin{cases} \frac{dS_c}{dt} &= \Pi_c + \sigma_1\xi R - (\mu_c + \delta_{cm} + \lambda_c + \gamma_c)S_c, \\ \frac{dS_m}{dt} &= \delta_{cm}S_c(1-\sigma_1-\sigma_2)\xi R - (\mu_m + \delta_{ma} + \lambda_m + \gamma_m)S_m, \\ \frac{dS_a}{dt} &= \delta_{ma}S_m + \sigma_2\xi R - (\mu_a + \delta_a + \gamma_a)S_a, \\ \frac{dE_c}{dt} &= \lambda_c S_c - (\mu_c + \tau_c + \gamma_c)E_c, \\ \frac{dE_m}{dt} &= \lambda_m S_m - (\mu_m + \tau_m + \gamma_m)E_m, \\ \frac{dE_a}{dt} &= \lambda_a S_a - (\mu_a + \tau_a + \gamma_a)E_a, \\ \frac{dI_c}{dt} &= \tau_c E_c - (\mu_c + d_c + \alpha_c + \gamma_c)I_c, \\ \frac{dI_m}{dt} &= \tau_m E_m - (\mu_m + d_m + \alpha_m + \gamma_m)I_m, \\ \frac{dI_a}{dt} &= \tau_a E_a - (\mu_a + d_a + \alpha_a + \gamma_a)I_a, \\ \frac{dT}{dt} &= \alpha_c I_c + \alpha_m I_m + \alpha_a I_a - (\mu_h + \gamma_h)T, \\ \frac{dR}{dt} &= \gamma_h T - (\mu_h + \phi)R, \\ \frac{dV_c}{dt} &= \gamma_c S_c - \mu_c V_c + \phi_1 R, \\ \frac{dV_m}{dt} &= \gamma_m S_m - \mu_m V_m + \phi_2 R, \\ \frac{dV_a}{dt} &= \gamma_a S_a - \mu_a V_a + \phi_3 R. \end{cases} \tag{B.1}$$

Now, we set the above equations of the system (B.1) equal to zero and solve these to find the equilibrium points. So, the equilibrium points are,

$$\begin{cases} E_0 = \left(S_c^0, S_m^0, S_a^0, 0, 0, 0, 0, 0, 0, 0, V_c^0, V_m^0, V_a^0\right); \\ S_c^0 = \frac{\Pi_c}{(\mu_c+\delta_{cm}+\gamma_c)}, S_m^0 = \frac{\Pi_c\delta_{cm}}{(\mu_c+\delta_{cm}+\gamma_c)(\mu_m+\delta_{ma}+\gamma_m)}, \\ S_a^0 = \frac{\Pi_c\delta_{cm}\delta_{ma}}{(\mu_a+\gamma_a)(\mu_c+\delta_{cm}+\gamma_c)(\mu_m+\delta_{ma}+\gamma_m)}, V_c^0 = \frac{\Pi_c\gamma_c}{\mu_c(\mu_c+\delta_{cm}+\gamma_c)}, \\ V_m^0 = \frac{\Pi_c\delta_m\gamma_m}{\mu_m(\mu_c+\delta_{cm}+\gamma_c)(\mu_m+\delta_{ma}+\gamma_m)}, V_a^0 = \frac{\Pi_c\delta_{cm}\delta_{ma}\gamma_a}{\mu_a(\mu_a+\gamma_a)(\mu_c+\delta_{cm}+\gamma_c)(\mu_m+\delta_{ma}+\gamma_m)}. \end{cases} \tag{B.2}$$

Theorem B.1. *The pneumonia transmission model for three different groups with vaccination (3.1) provides a unique disease-free equilibrium E_0.*

Proof. We may prove this theorem by substituting the disease-free equilibrium points E_0 into our introduced mathematical framework (3.1). After doing this evaluation, we find that the values of all derivatives are equal to zero. Hence, the desired result is proved. □

B.2 Endemic Equilibrium Points, E_1

Let the endemic equilibrium be

$$E_1 = \left(S_i^{**}, E_i^{**}, I_i^{**}, T^{**}, R^{**}, V_i^{**}\right), i = c, m, a,$$

which exists when the disease persists in the population and the equilibrium values are given analytically [27, 30, 33] as follows by setting

$$S_i^{**'} = E_i^{**'} = I_i^{**'} = T^{**'} = R^{**'} = V_i^{**'} = 0$$

Now, we the system algebraically to obtain the following expressions.
Exposed classes:

$$\begin{aligned} 0 &= \lambda_i S_i - (\mu_i + \tau_i + \gamma_i)E_i, \\ \Rightarrow \quad E_i^{**} &= \frac{\lambda_i S_i^{**}}{\mu_i + \tau_i + \gamma_i}, \quad i = c, m, a. \end{aligned}$$

Infected classes:

$$0 = \tau_i E_i - (\mu_i + d_i + \alpha_i + \gamma_i) I_i,$$
$$\Rightarrow \quad I_i^{**} = \frac{\tau_i E_i^{**}}{\mu_i + d_i + \alpha_i + \gamma_i}.$$

Substituting E_i^{**}, we obtain

$$I_i^{**} = \frac{\tau_i \lambda_i S_i^{**}}{(\mu_i + \tau_i + \gamma_i)(\mu_i + d_i + \alpha_i + \gamma_i)}, \quad i = c, m, a.$$

Treatment class:

$$0 = \alpha_c I_c + \alpha_m I_m + \alpha_a I_a - (\mu_h + \gamma_h) T,$$
$$\Rightarrow \quad T^{**} = \frac{\alpha_c I_c^{**} + \alpha_m I_m^{**} + \alpha_a I_a^{**}}{\mu_h + \gamma_h}.$$

Recovered class:

$$0 = \gamma_h T - (\mu_h + \phi) R,$$
$$\Rightarrow \quad R^{**} = \frac{\gamma_h T^{**}}{\mu_h + \phi}.$$

Substituting T^{**} gives

$$R^{**} = \frac{\gamma_h \left(\alpha_c I_c^{**} + \alpha_m I_m^{**} + \alpha_a I_a^{**}\right)}{(\mu_h + \gamma_h)(\mu_h + \phi)}.$$

Vaccinated classes:

$$0 = \gamma_i S_i - \mu_i V_i + \phi_1 R,$$
$$\Rightarrow \quad V_i^{**} = \frac{\gamma_i S_i^{**} + \phi_1 R^{**}}{\mu_i}, \quad i = c, m, a.$$

Susceptible classes:
For children:

$$0 = \Pi_c + \sigma_1 \xi R - (\mu_c + \delta_{cm} + \lambda_c + \gamma_c) S_c,$$
$$\Rightarrow \quad S_c^{**} = \frac{\Pi_c + \sigma_1 \xi R^{**}}{\mu_c + \delta_{cm} + \lambda_c + \gamma_c}.$$

For middle-aged individuals:

$$0 = \delta_{cm} S_c (1 - \sigma_1 - \sigma_2) \xi R - (\mu_m + \delta_{ma} + \lambda_m + \gamma_m) S_m,$$
$$\Rightarrow \quad S_m^{**} = \frac{\delta_{cm} S_c^{**} (1 - \sigma_1 - \sigma_2) \xi R^{**}}{\mu_m + \delta_{ma} + \lambda_m + \gamma_m}.$$

For adults:

$$0 = \delta_{ma} S_m + \sigma_2 \xi R - (\mu_a + \delta_a + \gamma_a) S_a,$$
$$\Rightarrow \quad S_a^{**} = \frac{\delta_{ma} S_m^{**} + \sigma_2 \xi R^{**}}{\mu_a + \delta_a + \gamma_a}.$$

Therefore, we get the following endemic equilibrium points E_1,

$$\begin{cases} E_i^{**} = \frac{\lambda_i S_i^{**}}{\mu_i + \tau_i + \gamma_i}, I_i^{**} = \frac{\tau_i \lambda_i S_i^{**}}{(\mu_i + \tau_i + \gamma_i)(\mu_i + d_i + \alpha_i + \gamma_i)}, \\ T^{**} = \frac{\sum_{i=c}^{m} \alpha_i I_i^{**}}{\mu_h + \gamma_h}, R^{**} = \frac{\gamma_h \sum_{i=c}^{m} \alpha_i I_i^{**}}{(\mu_h + \phi)(\mu_h + \gamma_h)}, V_i^{**} = \frac{\gamma_i S_i^{**} + \phi_1 R^{**}}{\lambda_i}, i = c, a, m, \\ S_c^{**} = \frac{\Pi_c + \sigma_1 \xi R^*}{\mu_c + \delta_{cm} + \lambda_c + \gamma_c}, S_m^{**} = \frac{\delta_{cm} S_c^{**} (1 - \sigma_1 - \sigma_2) \xi R^*}{\mu_m + \delta_{ma} + \lambda_m + \gamma_m}, S_a^{**} = \frac{\delta_{ma} S_m^{**} + \sigma_2 \xi R^*}{\mu_a + \lambda_a + \gamma_a}. \end{cases} \tag{B.3}$$

The endemic equilibrium E_1 represents a steady-state in which the disease persists in the population, characterized by non-zero exposed and infected compartments. The exposed and infected populations depend on the force of infection and progression rates, while they are reduced by recovery, vaccination, and death. The treatment and recovered classes reflect the effects of medical intervention and the development of temporary immunity. Moreover, the vaccinated population arises from both susceptible and recovered individuals, thereby contributing to the reduction of disease transmission. Overall, the equilibrium describes a balance between infection dynamics and control measures, typically occurring when $\mathcal{R}_0 > 1$.

B.3 Basic Reproduction Number (R_0)

Basic reproduction number serves as a threshold that determine whether an outbreak will grow or diminish based on whether R_0 exceeds or falls below unity. In biological models, if $R_0 > 1$, it implies disease spread and if $R_0 < 1$, it ensures the extinction of the disease. Using the next generation matrix, we acquire the basic reproduction number [33] of the model (3.1). To compute R_0, which entails determining the transition/transfer matrices, F and V as well as the spectral radius of FV^{-1}. Grouping the compartments of the infected individuals of system (3.1) and decomposing the right-hand-side as $F - V$, where F is the transmission part, we then express the generation of new infections and V the transition matrix. Therefore, we obtain the infectious compartments in the model and the relevant equations are:

$$F = \begin{pmatrix} \lambda_c S_c \\ \lambda_m S_m \\ \lambda_a S_a \\ 0 \\ 0 \\ 0 \end{pmatrix}; \quad V = \begin{pmatrix} (\mu_c + \tau_c)E_c \\ (\mu_m + \tau_m)E_m \\ (\mu_a + \tau_a)E_a \\ -\tau_c E_c + (\mu_c + d_c + \alpha_c)I_c \\ -\tau_m E_m + (\mu_m + d_m + \alpha_m)I_m \\ -\tau_a E_a + (\mu_a + d_a + \alpha_a)I_a \end{pmatrix}.$$

To find the transition matrix F, we use this formula,

$$F = \begin{pmatrix} \frac{\partial F_1}{\partial I_1} & \frac{\partial F_1}{\partial I_2} \\ \frac{\partial F_2}{\partial I_1} & \frac{\partial F_2}{\partial I_2} \end{pmatrix}.$$

For adding vaccination, we can find the transition matrix F and the transfer matrix V,

$$F = \begin{pmatrix} 0 & 0 & \frac{\beta_c S_c^o}{N_o} & \frac{\beta_m S_c^o}{N_o} & \frac{\beta_a S_c^o}{N_o} & 0 \\ 0 & 0 & \frac{\beta_c S_m^o}{N_o} & \frac{\beta_m S_m^o}{N_o} & \frac{\beta_a S_m^o}{N_o} & 0 \\ 0 & 0 & \frac{\beta_c S_a^o}{N_o} & \frac{\beta_m S_a^o}{N_o} & \frac{\beta_a S_a^o}{N_o} & 0 \\ 0 & 0 & 0 & 0 & 0 & 0 \\ 0 & 0 & 0 & 0 & 0 & 0 \\ 0 & 0 & 0 & 0 & 0 & 0 \end{pmatrix},$$

and

$$V = \begin{pmatrix} g_1 & 0 & 0 & 0 & 0 & 0 \\ 0 & g_2 & 0 & 0 & 0 & 0 \\ 0 & 0 & g_3 & 0 & 0 & 0 \\ -\tau_c & 0 & 0 & g_4 & 0 & 0 \\ 0 & -\tau_m & 0 & 0 & g_5 & 0 \\ 0 & 0 & -\tau_a & 0 & 0 & g_6 \end{pmatrix}.$$

For simplicity, we let, $g_1 = \mu_c + \tau_c + \gamma_c$; $g_2 = \mu_m + \tau_m + \gamma_m$; $g_3 = \mu_a + \tau_a + \gamma_a$; $g_4 = \mu_c + d_c + \alpha_c + \gamma_c$; $g_5 = \mu_m + d_m + \alpha_m + \gamma_m$; $g_6 = \mu_a + d_a + \alpha_a + \gamma_a$.

Let, $A_1 = \frac{S_c^o}{N_o}$, $A_2 = \frac{S_m^o}{N_o}$, $A_3 = \frac{S_a^o}{N_o}$. To find the spectral radius, we compute,

$$FV^{-1} = \begin{pmatrix} \frac{\beta_c A_1 \tau_c}{g_1 g_4} & \frac{\beta_c A_1 \tau_m}{g_2 g_5} & \frac{\beta_c A_1 \tau_a}{g_3 g_6} & \frac{\beta_c A_1}{g_4} & \frac{\beta_c A_1}{g_5} & \frac{\beta_c A_1}{g_6} \\ \frac{\beta_m A_2 \tau_c}{g_1 g_4} & \frac{\beta_m A_2 \tau_m}{g_2 g_5} & \frac{\beta_m A_2 \tau_m}{g_3 g_6} & \frac{\beta_m A_2}{g_4} & \frac{\beta_m A_2}{g_5} & \frac{\beta_m A_2}{g_6} \\ \frac{\beta_a A_3 \tau_c}{g_1 g_4} & \frac{\beta_a A_3 \tau_m}{g_2 g_5} & \frac{\beta_a A_3 \tau_a}{g_3 g_6} & \frac{\beta_a A_3}{g_4} & \frac{\beta_a A_3}{g_5} & \frac{\beta_a A_3}{g_6} \\ 0 & 0 & 0 & 0 & 0 & 0 \\ 0 & 0 & 0 & 0 & 0 & 0 \\ 0 & 0 & 0 & 0 & 0 & 0 \end{pmatrix}. \tag{B.4}$$

Now, the basic reproduction number is

$$R_0 = R_c + R_m + R_a = \frac{\beta_c \tau_c A_1}{g_1 g_4} + \frac{\beta_m \tau_m A_2}{g_2 g_5} + \frac{\beta_a \tau_a A_3}{g_3 g_6}.$$

$$\begin{cases} g_1 &= \mu_c + \tau_c + \gamma_c, \\ g_2 &= \mu_m + \tau_m + \gamma_m, \\ g_3 &= \mu_a + \tau_a + \gamma_a, \\ g_4 &= \mu_c + d_c + \alpha_c + \gamma_c, \\ g_5 &= \mu_m + d_m + \alpha_m + \gamma_m, \\ g_6 &= \mu_a + d_a + \alpha_a + \gamma_a. \end{cases}$$

$$\begin{cases} g_1 g_4 &= (\mu_c + \tau_c + \gamma_c)(\mu_c + d_c + \alpha_c + \gamma_c) = 0.877340602, \\ g_2 g_5 &= (\mu_m + \tau_m + \gamma_m)(\mu_m + d_m + \alpha_m + \gamma_m) = 0.03288922616, \\ g_3 g_6 &= (\mu_a + \tau_a + \gamma_a)(\mu_a + d_a + \alpha_a + \gamma_a) = 0.2114931246. \end{cases}$$

Let $S_c^o = 2000$; $S_m^o = 300$; $S_a^o = 2000$; $N_o = 5250$. Then,

$$F = \begin{pmatrix} \frac{\partial}{\partial I_c}\left(\frac{\partial I_c}{\partial t}\right) & \frac{\partial}{\partial I_m}\left(\frac{\partial I_c}{\partial t}\right) & \frac{\partial}{\partial I_a}\left(\frac{\partial I_c}{\partial t}\right) \\ \frac{\partial}{\partial I_c}\left(\frac{\partial I_m}{\partial t}\right) & \frac{\partial}{\partial I_m}\left(\frac{\partial I_m}{\partial t}\right) & \frac{\partial}{\partial I_a}\left(\frac{\partial I_m}{\partial t}\right) \\ \frac{\partial}{\partial I_c}\left(\frac{\partial I_a}{\partial t}\right) & \frac{\partial}{\partial I_m}\left(\frac{\partial I_a}{\partial t}\right) & \frac{\partial}{\partial I_a}\left(\frac{\partial I_a}{\partial t}\right) \end{pmatrix}.$$

After completing respective calculations, we get

$$F = \begin{pmatrix} -(\mu_c + d_c + \alpha_c + \gamma_c) & 0 & 0 \\ 0 & -(\mu_m + d_m + \alpha_m + \gamma_m) & 0 \\ 0 & 0 & -(\mu_a + d_a + \alpha_a + \gamma_a) \end{pmatrix}.$$

Characteristic equation: $|F - \lambda I| = 0$,

$$\Rightarrow \begin{vmatrix} -(\mu_c + d_c + \alpha_c + \gamma_c + \lambda) & 0 & 0 \\ 0 & -(\mu_m + d_m + \alpha_m + \gamma_m + \lambda) & 0 \\ 0 & 0 & -(\mu_a + d_a + \alpha_a + \gamma_a + \lambda) \end{vmatrix} = 0,$$

$$\Rightarrow -(\mu_c + d_c + \alpha_c + \gamma_c + \lambda)(\mu_m + d_m + \alpha_m + \gamma_m + \lambda)(\mu_a + d_a + \alpha_a + \gamma_a + \lambda) = 0.$$

Then,

$$\begin{cases} \lambda_1 &= -(\mu_c + d_c + \alpha_c + \gamma_c) = -0.8652338421, \\ \lambda_2 &= -(\mu_m + d_m + \alpha_m + \gamma_m) = -0.06204936443, \\ \lambda_3 &= -(\mu_a + d_a + \alpha_a + \gamma_a) = -0.2577769863. \end{cases}$$

For vaccination, the basic reproduction number becomes, $R_0 = 0.1197229 + 0.14090712 + 0.03787183156 \approx 0.298$.

Theorem B.2. *Consider the system (3.1), which represents a pneumonia transmission model for three different age groups with vaccination.*

1. *The disease-free equilibrium (DFE), E_0, of the study (3.1), is locally asymptotically stable when $R_0 < 1$.*
2. *The disease-free equilibrium (DFE), E_0 of the system (3.1), is unstable if the fundamental reproduction number $R_0 > 1$. Hence, there exists a unique endemic equilibrium, E_1.*

Proof. The proof of this theorem is determined by considering two cases. Here, we analyze the stability of the disease-free equilibrium (DFE) E_0 by applying the next-generation matrix method together with Jacobian stability theory. Let the system's (3.1) infected compartments are divided as:

$$X = (E_c, E_m, E_a, I_c, I_m, I_a)^T.$$

Equation (B.4) represents the next-generation matrix and the basic reproduction number [33] is defined as:

$$R_0 = \rho(FV^{-1}), \qquad \text{where } \rho(\cdot) \text{ denotes the spectral radius.}$$

Next, we get a linearized infected subsystem at the disease-free equilibrium E_0, which is given by:

$$\frac{dX}{dt} = (F - V)X.$$

This can be rewritten as: $F - V = V(FV^{-1} - I)$. were, V is a non-singular M-matrix, since V is a Metzler matrix with strictly positive diagonal entries and all off-diagonal entries non-positive, and each diagonal entry exceeds the sum of the corresponding off-diagonal magnitudes. Hence, V is invertible and also its inverse is non-negative. Therefore, the eigenvalue structure of $F - V$ is determined by that of $FV^{-1} - I$. Particularly, the spectral radius $\rho(FV^{-1})$ is used to identify the the sign of the real parts of the eigenvalues of $J(E_0)$.

Case 1: $R_0 < 1$**.** If $R_0 < 1$, then $\rho(FV^{-1}) < 1$, which implies that all eigenvalues of $FV^{-1} - I$ have negative real parts. Hence, all eigenvalues of both $F - V$ and $J(E_0)$ (B.5) are negative in real part. Therefore, the disease-free equilibrium E_0 is locally asymptotically stable based on the next-generation theorem formulated by van den Driessche and Watmough (2002) [33].

Case 2: $R_0 > 1$**.** If $R_0 > 1$, then $\rho(FV^{-1}) > 1$, implying that $FV^{-1} - I$ possesses at least one eigenvalue with positive real part. Consequently, both $F - V$ and $J(E_0)$ (B.5) have at least one eigenvalue with positive real part. This means that the DFE E_0, is not stable in the area. So, when $R_0 > 1$, the equilibrium equations give a single biologically feasible solution, which is represented by the equation (B.3). The infected compartments are non-negative, supported by the equation (3.2). So, we can say that there exists a unique endemic equilibrium E_1 in the admissible physiological domain for the system (3.1). □

B.4 Local and Global Stability Analysis

At the disease-free equilibrium (DFE), the local stability of system (3.1) is analyzed, that is $E_0 = \Big(\frac{\Pi_c}{(\mu_c+\delta_{cm}+\gamma_c)}, \frac{\Pi_c\delta_{cm}}{(\mu_c+\delta_{cm}+\gamma_c)(\mu_m+\delta_{ma}+\gamma_m)}, \frac{\Pi_c\delta_{cm}\delta_{ma}}{(\mu_a+\gamma_a)(\mu_c+\delta_{cm}+\gamma_c)(\mu_m+\delta_{mg}+\gamma_m)}, 0, 0, 0, 0, 0, 0, 0, 0, 0, \frac{\Pi_c\gamma_c}{\mu_c(\mu_c+\delta_{cm}+\gamma_c)}, \frac{\Pi_c\delta_m\gamma_m}{\mu_m(\mu_c+\delta_{cm}+\gamma_c)(\mu_m+\delta_{ma}+\gamma_m)}, \frac{\Pi_c\delta_{cm}\delta_{ma}\gamma_a}{\mu_a(\mu_a+\gamma_a)(\mu_c+\delta_{cm}+\gamma_c)(\mu_m+\delta_{ma}+\gamma_m)}\Big)$ is determined according to the eigenvalues using Jacobian matrix. The Jacobian matrix of (3.1) is therefore,

$$J(E_0) = \begin{bmatrix}
a_{11} & 0 & 0 & 0 & 0 & 0 & 0 & 0 & 0 & 0 & 0 & 0 & 0 & 0 \\
a_{21} & a_{22} & 0 & 0 & 0 & 0 & 0 & 0 & 0 & 0 & 0 & 0 & 0 & 0 \\
0 & a_{32} & a_{33} & 0 & 0 & 0 & 0 & 0 & 0 & 0 & 0 & 0 & 0 & 0 \\
a_{41} & 0 & 0 & a_{44} & 0 & 0 & 0 & 0 & 0 & 0 & 0 & 0 & 0 & 0 \\
0 & a_{52} & 0 & 0 & a_{55} & 0 & 0 & 0 & 0 & 0 & 0 & 0 & 0 & 0 \\
0 & 0 & a_{63} & 0 & 0 & a_{66} & a_{67} & 0 & 0 & 0 & 0 & 0 & 0 & 0 \\
0 & 0 & 0 & \tau_p & 0 & 0 & 0 & a_{78} & 0 & 0 & 0 & 0 & 0 & 0 \\
0 & 0 & 0 & 0 & \tau_m & 0 & 0 & 0 & a_{89} & 0 & 0 & 0 & 0 & 0 \\
0 & 0 & 0 & 0 & 0 & \tau_g & \alpha_p & \alpha_m & \alpha_g & -(\mu_h+\gamma_h) & 0 & 0 & 0 & 0 \\
0 & 0 & 0 & 0 & 0 & 0 & 0 & 0 & 0 & \gamma_h & -(\mu_1+\phi) & 0 & 0 & 0 \\
0 & 0 & 0 & 0 & 0 & 0 & 0 & 0 & 0 & 0 & \phi_1 & -\mu_p & 0 & 0 \\
0 & 0 & 0 & 0 & 0 & 0 & 0 & 0 & 0 & 0 & \phi_2 & 0 & -\mu_m & 0 \\
0 & 0 & 0 & 0 & 0 & 0 & 0 & 0 & 0 & 0 & \phi_3 & 0 & 0 & -\mu_g
\end{bmatrix}. \tag{B.5}$$

where $a_{11} = -(\mu_c + \delta_{cm} + \lambda_c + \gamma_c)$, $a_{21} = \delta_{cm}(1-\beta_m)(1-H_m)(1-\sigma_1-\sigma_2)\epsilon R$, $a_{22} = -(\mu_c + \delta_{cm} + \lambda_c + \gamma_c)$, $a_{32} = \delta_{ma}$, $a_{33} = -(\mu_a + \lambda_a + \gamma_a)$, $a_{41} = \lambda_c(1-H_c)(1-\beta_c)$, $a_{44} = -(\mu_c + \tau_c + \gamma_c)$, $a_{52} = \lambda_m(1-H_m)(1-\beta_m)$, $a_{55} = -(\mu_m + \tau_m + \gamma_m)$, $a_{63} = \lambda_a(1-H_a)(1-\beta_a)$, $a_{66} = -(\mu_a + \tau_a + \gamma_a)$, $a_{67} = -(\mu_c + d_c + \alpha_c + \gamma_c)$, $a_{78} = -(\mu_m + d_m + \alpha_m + \gamma_m)$, and $a_{89} = -(\mu_a + d_a + \alpha_a + \gamma_a)$.

In our developed pneumonia spread model (3.1), we obtain the eigenvalue in the form $-a+ib$, which is a complex value. Here, the imaginary part of the value is positive and the real part is negative. So, the study is locally stable in the asymptotic sense. Hence, our modified pneumonia transmission model with vaccination is locally stable in the asymptotic sense at the equilibrium points.

Theorem B.3. *The proposed model (3.1) is locally stable in the asymptotic sense at the DFE, E_0.*

Proof. At the DFE, the local stability of the proposed pneumonia transmission model (3.1), E_0 depends on the eigenvalues of the Jacobian matrix, $J(E_0)$ (B.5) [30], [33], while the characteristic equation is

$$\det\big(J(E_0) - \lambda I\big) = 0. \tag{B.6}$$

For the model (3.1), the Jacobian matrix $J(E_0)$ is a lower block-triangular matrix. Hence, we take the product of the determinants of its diagonal blocks for calculating the characteristic equation (B.6). Sequentially, the eigenvalues of each diagonal block provide the eigenvalues of $J(E_0)$. Then, the following eigenvalues can be obtained directly from the demographic and immunization blocks.

$$\begin{aligned}
&\lambda_1 = -(\mu_c + \delta_{cm} + \gamma_c), \quad \lambda_2 = -(\mu_m + \delta_{ma} + \gamma_m),\\
&\lambda_3 = -(\mu_a + \gamma_a), \quad \lambda_4 = -(\mu_h + \gamma_h), \quad \lambda_5 = -(\mu_h + \phi),\\
&\lambda_6 = -\mu_c, \quad \lambda_7 = -\mu_m, \quad \lambda_8 = -\mu_a,
\end{aligned}$$

where all of them are strictly negative. Next, from the infected subsystem, the remaining eigenvalues are $E_c, E_m, E_a, I_c, I_m, I_a$. That subsystem break downs into three independent blocks, which are 2×2 and corresponds to individuals under 5 years, 5–64 years, and above 64 years. Now, the characteristic equation connected to the respective block for each age group $i \in \{c, m, a\}$ is

$$\det\begin{pmatrix} -(\mu_i + \tau_i + \gamma_i) - \lambda & 0 \\ \tau_i & -(\mu_i + d_i + \alpha_i + \gamma_i) - \lambda \end{pmatrix} = 0,$$

which implies that

$$\lambda^2 + D_i\lambda + P_i = 0, \tag{B.7}$$

where $D_i = (\mu_i + \tau_i + \gamma_i) + (\mu_i + d_i + \alpha_i + \gamma_i)$ and for epidemiological interpretation rewrite P_i as $P_i = (\mu_i + \tau_i + \gamma_i)(\mu_i + d_i + \alpha_i + \gamma_i)(1 - R_i)$. Now, according to Routh-Hurwitz criterion [30], all roots of the quadratic characteristic equation (B.7) have negative real parts if and only if $D_i > 0 \quad \text{and} \quad P_i > 0$. Since $R_i < 1$ and all parameters are positive, it is obvious that $D_i, P_i > 0$, always holds. Eventually, the calculated value of $R_0 = R_c + R_m + R_a < 1$, so that all eigenvalues of $J(E_0)$ contain negative real parts and the model *(3.1)* is locally stable in the asymptotic sense at the DFE, E_0. □

Theorem B.4. *Suppose the pneumonia framework (3.1) including vaccination classes for three different age groups.*

1. *If $R_0 < 1$, the disease-free equilibrium (DFE), E_0, of system (3.1) is globally asymptotically stable.*
2. *If $R_0 > 1$, the endemic equilibrium, E_1, of system (3.1) is globally asymptotically stable.*

Proof. The proposition is proved consisting of two sections, and we apply proper Lyapunov functions and LaSalle's Invariance Principle [34] for doing this. The disease-free equilibrium (DFE) of the system (3.1) is represented by the equation (B.2), as well as the steady-state equilibrium E_1 of system (3.1) is represented by the equation (B.3).

For the first part, let us consider that $R_0 < 1$. Here, at the DFE E_0, all compartments which are infected are considered to be zero, i.e., $E_c = E_m = E_a = I_c = I_m = I_a = T = R = 0$. Hence, the Lyapunov function at the DFE is described as,

$$L = \sum_{i=c,m,a} \left(\frac{E_i}{g_j} + \frac{I_i}{g_{j+3}} \right) + \frac{T}{\mu_h + \gamma_h} + \frac{R}{\mu_h + \phi}, \ j = 1, 2, 3, \tag{B.8}$$

where $g_j = \mu_i + \tau_i + \gamma_i$ and $g_{j+3} = \mu_i + d_i + \alpha_i + \gamma_i$, with $j = 1, 2, 3$.

We construct the Lyapunov function L based on the structure of the infectious compartments of the system. Since the disease dynamics are governed by the exposed (E_i), infected (I_i), treatment (T), and recovered (R) classes, the Lyapunov function L is defined as a linear combination of these state variables. In addition, the corresponding total removal rates from each compartment are used to normalize L. In particular, $g_{j+3} = \mu_i + d_i + \alpha_i + \gamma_i$ represents the total removal rate from the infected class I_i, and $g_j = \mu_i + \tau_i + \gamma_i$ denotes the total rate at which individuals leave the exposed class E_i. Similarly, $(\mu_h + \phi)$ and $(\mu_h + \gamma_h)$ represent the total removal rates from the recovered and treatment compartments, respectively. This normalization ensures that each term in the Lyapunov function has comparable scaling and reflects the average duration spent in each compartment.

Since all state variables are non-negative, the function L is positive definite in the feasible region, and $L = 0$ if and only if $E_i = I_i = T = R = 0$, which corresponds to the disease-free equilibrium E_0. Therefore, the constructed Lyapunov function L effectively captures the total infectious burden of the system and is suitable for analyzing the global stability of the disease-free equilibrium.

Then, differentiating the Lyapunov function (B.8) with respect to the system trajectories, we obtain:

$$\begin{aligned}
\frac{dL}{dt} &= \sum_{i=c,m,a} \left(\frac{E_i'}{g_j} + \frac{I_i'}{g_{j+3}} \right) + \frac{T'}{\mu_h + \gamma_h} + \frac{R'}{\mu_h + \phi} \\
&= \sum_{i=c,m,a} \frac{\lambda_i S_i^0 - g_j E_i}{g_j} + \frac{\tau_i E_i - g_{j+3} I_i}{g_{j+3}} + \frac{\sum_i \alpha_i I_i - (\mu_h + \gamma_h) T}{\mu_h + \gamma_h} + \frac{\gamma_h T - (\mu_h + \phi) R}{\mu_h + \phi} \\
&= \sum_{i=c,m,a} \frac{\lambda_i S_i^0}{g_j} - \sum_{i=c,m,a} (E_i + I_i) \\
&\leq \sum_{i=c,m,a} R_i I_i - \sum_{i=c,m,a} I_i \\
&= (R_0 - 1) \sum_{i=c,m,a} I_i \leq 0,
\end{aligned}$$

where $R_i = \frac{\beta_i \tau_i A_j}{g_j g_{j+3}}$.

We apply LaSalle's invariance principle to analyze the global stability of the disease-free equilibrium. From the above calculations, we find that $\frac{dL}{dt} \leq 0$ for $R_0 < 1$, and the equality $\frac{dL}{dt} = 0$ holds for $E_i = I_i = T = R = 0$, which corresponds to the disease-free equilibrium E_0. Hence, the largest invariant set contained in $\left\{ \frac{dL}{dt} = 0 \right\}$ is the singleton $\{E_0\}$. Therefore, LaSalle's invariance principle confirms that all solutions starting in the feasible region approach E_0 as $t \to \infty$, which indicates that all infected compartments vanish asymptotically and the system approaches a steady state in which no disease persists in the population. Since, in the feasible region, the convergence holds for any initial condition, E_0 is not only stable but also attracts all trajectories globally. Consequently, it is proved that the disease-free equilibrium E_0 of system (3.1) is globally asymptotically stable whenever $R_0 < 1$.

Next, start for the second part and consider $R_0 > 1$, for which a unique endemic equilibrium (B.3) exists. In this stage, we introduce a Lyapunov function of Volterra-type and presented by the equation (B.9),

$$\begin{aligned}
L_v = \sum_i \Bigg[E_i - E_i^{**} - E_i^{**} \ln \frac{E_i}{E_i^{**}} + I_i - I_i^{**} - I_i^{**} \ln \frac{I_i}{I_i^{**}} \Bigg] \\
+ T - T^{**} - T^{**} \ln \frac{T}{T^{**}} + R - R^{**} - R^{**} \ln \frac{R}{R^{**}}
\end{aligned} \tag{B.9}$$

were, a Volterra-type (logarithmic) functional form is used for contructing the Lyapunov function L_v, which have a common use in epidemic models to analyze global stability of endemic equilibria and this

Lyapunov function L_v is formed based on the relative entropy structure:

$$V(z, z^*) = z - z^{**} - z^{**} \ln\left(\frac{z}{z^{**}}\right), \quad z, z^{**} > 0, \tag{B.10}$$

which is non-negative for all $z, z^{**} > 0$ and becomes zero if and only if $z = z^{**}$. This structure measures the deviation of the current state from the endemic equilibrium in a nonlinear but positive definite manner and due to this reason it is particularly suitable for biological systems. Moreover, when $\frac{dL_v}{dt} \leq 0$, a crucial situation occurs and its logarithmic form allows cancellation with equilibrium relations. Therefore, for establishing the global stability of the endemic equilibrium, a natural candidate Lyapunov function is constructed by the sum of such terms over all compartments.

Since, it is obvious that for any $z, z^{**} > 0$, the inequality $z - z^{**} - z^{**} \ln\left(\frac{z}{z^{**}}\right) \geq 0$ is always true, hence, $L_v \geq 0$ for all (E_i, I_i, T, R) and $L_v = 0$ if and only if $(E_i, I_i, T, R) = (E_i^{**}, I_i^{**}, T^{**}, R^{**})$ at E_1. Now, take the derivative of L_v along the system trajectories. However, the time derivative of a Volterra-type term of the form (B.10) is given by:

$$\frac{d}{dt}\left(z - z^{**} - z^{**} \ln\frac{z}{z^{**}}\right) = \left(1 - \frac{z^{**}}{z}\right)\frac{dz}{dt}.$$

Applying this result to each compartment variable E_i, I_i, T, and R, and summing over all indices i, we obtain

$$\begin{aligned}\frac{dL_v}{dt} = &\sum_i \left(1 - \frac{E_i^{**}}{E_i}\right)\frac{dE_i}{dt} + \sum_i \left(1 - \frac{I_i^{**}}{I_i}\right)\frac{dI_i}{dt} \\ &+ \left(1 - \frac{T^{**}}{T}\right)\frac{dT}{dt} + \left(1 - \frac{R^{**}}{R}\right)\frac{dR}{dt}.\end{aligned} \tag{B.11}$$

Now, we substitute the model equations into (B.11) and apply the equilibrium relations at E_1 (B.3). For example, for the exposed class, we have $E_i' = \lambda_i S_i - g_i E_i$, where $g_i = \mu_i + \tau_i + \gamma_i$. At the endemic equilibrium, $\lambda_i S_i^{**} = g_i E_i^{**}$. Thus,

$$E_i' = \lambda_i(S_i - S_i^{**}) - g_i(E_i - E_i^{**}).$$

Multiplying by $\left(1 - \frac{E_i^{**}}{E_i}\right)$, we obtain

$$\left(1 - \frac{E_i^{**}}{E_i}\right)E_i' = \left(1 - \frac{E_i^{**}}{E_i}\right)\left[\lambda_i(S_i - S_i^{**}) - g_i(E_i - E_i^{**})\right],$$

which contains the term $(E_i - E_i^{**})\left(1 - \frac{E_i^{**}}{E_i}\right)$. Similar derivations hold for all other compartments.

Therefore, each component of $\frac{dL_v}{dt}$ can be written in the form

$$(z - z^{**})\left(1 - \frac{z^{**}}{z}\right), \quad z > 0.$$

For $z > 0$, this expression is non-positive and attains zero if and only if $z = z^{**}$. Hence, it follows that $\frac{dL_v}{dt} \leq 0$. Moreover, $\frac{dL_v}{dt} = 0$ holds if and only if

$$E_i = E_i^{**}, \quad I_i = I_i^{**}, \quad T = T^{**}, \quad R = R^{**}.$$

Thus, the largest invariant set contained in $\left\{\frac{dL_v}{dt} = 0\right\}$ reduces to the singleton $\{E_1\}$. Consequently, by LaSalle's invariance principle, all solutions of system (3.1) starting in the feasible region converge to the endemic equilibrium E_1 as $t \to \infty$. Therefore, the endemic equilibrium is globally asymptotically stable whenever $R_0 > 1$.

□

Hence, we can summarize that when $R_0 < 1$, the disease dies out in all age groups and the DFE, E_0 is globally asymptotically stable. Conversely, when $R_0 > 1$, then endemic equilibrium, E_1 exists and the infection persists in the community at a stable level.

From Theorem B.4, we obtain a clear threshold characterization of the model dynamics. It is shown that if $R_0 < 1$, the disease-free equilibrium E_0 is globally asymptotically stable, indicating that the disease dies out in all age groups regardless of the initial number of infections as $t \to \infty$. However, if $R_0 > 1$, the system converges to a unique endemic equilibrium E_1 as $t \to \infty$, implying that the disease persists in the population at a stable endemic level. This demonstrates that, under the proposed vaccination and treatment strategies, R_0 acts as a threshold parameter governing the elimination or persistence of pneumonia in the long-term dynamics of the system.

References

[1] Mayo Clinic. (2026). Infectious diseases: Symptoms & causes. Retrieved January 2026, from https://www.mayoclinic.org/diseases-conditions/infectious-diseases/symptoms-causes/syc-20351173

[2] Akter, M., Alam, M., & Kamrujjaman, M. (2024). An in-silico game theoretic approach to study the efficacy of several health interventions to appease the rapid transmission of multi-strained epidemics. Healthcare Analytics, 6, 100318. https://doi.org/10.1016/j.health.2024.100318

[3] World Health Organization. (2026). Global Health Observatory (GHO) data repository. Retrieved January 2026, from https://www.who.int/data/gho

[4] Centers for Disease Control and Prevention. (2026). About pneumonia: Causes, types, and common pathogens. Retrieved January 2026, from https://www.cdc.gov/pneumonia/about/index.html

[5] Our World in Data. (2026). Pneumonia. Retrieved January 2026, from https://ourworldindata.org/pneumonia

[6] UNICEF. (2026). Pneumonia in children: Statistics. UNICEF Data. Retrieved January 2026, from https://data.unicef.org/topic/child-health/pneumonia/

[7] Directorate General of Health Services. (2026). Official portal of the Directorate General of Health Services. Government of Bangladesh. Retrieved January 2026, from https://dghs.gov.bd/

[8] Jacobs, M. R. (2004). Streptococcus pneumoniae: Epidemiology and patterns of resistance. *American Journal of Medicine*, *117*(3), 3–15. https://doi.org/10.1016/j.amjmed.2004.07.003

[9] Kosasih, K., Abeyratne, U. R., Swarnkar, V., & Triasih, R. (2015). Wavelet augmented cough analysis for rapid childhood pneumonia diagnosis. *IEEE Transactions on Biomedical Engineering*, *62*(4), 1185–1194. https://doi.org/10.1109/tbme.2014.2381214

[10] Ngari, C., Pokhariyal, G., & Koske, J. (2016). Analytical model for childhood pneumonia: A case study of Kenya. *British Journal of Mathematics & Computer Science*, *12*(2), 1–28. https://doi.org/10.9734/BJMCS/2016/20180

[11] Wardlaw, T., Salama, P., Johansson, E. W., & Mason, E. (2006). Pneumonia: the leading killer of children. *The Lancet*, 368 (9541), 1048–1050. https://doi.org/10.1016/s0140-6736(06)69334-3

[12] Idowu, K. O. & Erinle-Ibrahim, L. M. (2021). Mathematical modeling of pneumonia dynamics of children under the age of five. *PREPRINT (Version 1) available at Research Square.* https://doi.org/10.21203/rs.3.rs-194578/v1

[13] Lamb, K. E., Greenhalgh, D. , & Robertson, C. (2011). A simple mathematical model for genetic effects in pneumococcal carriage and transmission. *Journal of Computational and Applied Mathematics*, 235(7), 1812–1818. https://doi.org/10.1016/j.cam.2010.03.019

[14] Kosasih, K., & Abeyratne, U. (2017). Exhaustive mathematical analysis of simple clinical measurements for childhood pneumonia diagnosis. *World Journal of Pediatrics*, *13*(5), 446–456. https://doi.org/10.1007/s12519-017-0019-4

[15] Tilahun, G. T., Makinde, O. D., & Malonza, D. (2017). Modeling and optimal control of pneumonia disease with cost-effective strategies. *Journal of Biological Dynamics*, *11*(2), 400–426. https://doi.org/10.1080/17513758.2017.1337245

[16] Kizito, M., & Tumwiine, J. (2018). A mathematical model of treatment and vaccination interventions of pneumococcal pneumonia infection dynamics. *Journal of Applied Mathematics*, *2018*, Article ID 2539465. https://doi.org/10.1155/2018/2539465

[17] Diah, I. M., & Aziz, N. (2019). Stochastic modeling for pneumonia incidence: A conceptual framework. In *AIP Conference Proceedings*, 1, 1–3. https://doi.org/10.1063/1.5121115

[18] Santos, G., & Vera, J. (2020). The role of age, neutrophil infiltration and antibiotics timing in the severity of Streptococcus pneumoniae pneumonia: insights from a multi-level mathematical model approach. *International Journal of Molecular Sciences*, *21*(22), 8428. https://doi.org/10.3390/ijms21228428

[19] Zephaniah, O. C., Nwaugonma, U. I. R., Chioma, I. S., & Adrew, O. (2020). A mathematical model and analysis of an SVEIR model for Streptococcus pneumonia with saturated incidence force of infection. *Mathematical Modeling and Applications*, *5*(1), 16–38. https://doi.org/10.11648/j.mma.20200501.13

[20] Otoo, D., Opoku, P., Charles, S., & Kingsley, A. P. (2020). Deterministic epidemic model for (SVCSyCAsyIR) pneumonia dynamics, with vaccination and temporal immunity. *Infectious Disease Modeling*, *5*, 42–60. https://doi.org/10.1016/j.idm.2019.11.001

[21] Ouwatobi, K. I., & Erinle-Ibrahim, L. M. (2021). Mathematical modeling of pneumonia dynamics of children under the age of five. *Research Square (preprint)*. https://doi.org/10.21203/rs.3.rs-194578/v1

[22] Wafula, N. M., Kwach, B. O., & Marani, V. N. (2021). Mathematical modeling and optimal control for controlling pneumonia-HIV coinfection. *International Journal of Innovative Research and Development*, *10*(1), 138–144. https://doi.org/10.24940/ijird/2021/v10/i1/JAN21051

[23] Naveed, M., et al. (2021). Modeling the transmission dynamics of delayed pneumonia-like diseases with a sensitivity of parameters. *Advances in Difference Equations*, *2021*(1), 468. https://doi.org/10.1186/s13662-021-03618-z

[24] Aldila, D., Hassan, A. H., Aziz, M. H. N., & Kamalia, P. Z. (2025). An analytical transmission model for evaluating pneumonia vaccination and control strategies. Healthcare Analytics, 7, 100394. https://doi.org/10.1016/j.health.2025.100394

[25] Horn, M., Theilacker, C., Sprenger, R., von Eiff, C., Mahar, E., Schiffner-Rohe, J., et al. (2023). Mathematical modeling of pneumococcal transmission dynamics in response to PCV13 infant vaccination in Germany predicts increasing IPD burden due to serotypes included in next-generation PCVs. *PLoS ONE*, *18*(2), e0281261. https://doi.org/10.1371/journal.pone.0281261

[26] Shyamsunder, S., & Purohit, S. D. (2024). A novel study of the impact of vaccination on pneumonia via fractional approach. *Partial Differential Equations in Applied Mathematics*, *10*, 100698. https://doi.org/10.1016/j.padiff.2024.100698

[27] Chukwu, C. W., Tchoumi, S. Y., & Diagne, M. L. (2024). A simulation study to assess the epidemiological impact of pneumonia transmission dynamics in high-risk populations. *Decision Analytics Journal*, *10*, 100423. https://doi.org/10.1016/j.dajour.2024.100423

[28] World Health Organization. (2025, May 28). *Pneumonia*. retrieved from https://www.who.int/news-room/fact-sheets/detail/pneumonia.

[29] Kobayashi, M. (2025). Expanded recommendations for use of pneumococcal conjugate vaccines among adults aged≥ 50 years: recommendations of the Advisory Committee on Immunization Practices—United States, 2024. MMWR. Morbidity and Mortality Weekly Report, 74. https://www.cdc.gov/mmwr/volumes/74/wr/mm7401a1.htm

[30] Mayeda, K., Lima, S. A., Ullah, A., & Kamrujjaman, M. (2026). Can dengue be controlled? Assessing vaccination and insecticide strategies with optimal control. *Alexandria Engineering Journal*, 134, 508-525. https://doi.org/10.1016/j.aej.2025.12.039

[31] Aseev, S. M., & Kryazhimskiy, A. V. (2007). The Pontryagin maximum principle and optimal economic growth problems. *Proceedings of the Steklov Institute of Mathematics*, 257(1), 1–255. https://doi.org/10.1134/S0081543807020010

[32] Blower, S. M., & Dowlatabadi, H. (1994). Sensitivity and uncertainty analysis of complex models of disease transmission: An HIV model, as an example. *International Statistical Review*, 62(2), 229–243. https://doi.org/10.2307/1403510

[33] Van den Driessche, P., & Watmough, J. (2002). Reproduction numbers and sub-threshold endemic equilibria for compartmental models of disease transmission. *Mathematical Biosciences*, 180, 29–48. https://doi.org/10.1016/S0025-5564(02)00108-6

[34] Salle, J. L., & Lefschetz, S. (1961). Stability by Liapunov's direct method with applications, *Academic Press, New York*.